


## Quantification of fluctuations from fluorescence correlation spectroscopy experiments in reaction-diffusion systems

Cecilia Villarruel<sup>1,2,\*</sup> and Silvina Ponce Dawson<sup>1</sup>

<sup>1</sup>*Departamento de Física, FCEN-UBA, and IFIBA, UBA-CONICET, Ciudad Universitaria, Pabellón I, Buenos Aires, Argentina*

<sup>2</sup>*IFIBYNE, UBA-CONICET, Buenos Aires, Argentina*

 (Received 19 November 2019; revised 8 May 2020; accepted 12 October 2020; published 12 November 2020)

Fluorescence correlation spectroscopy (FCS) is commonly used to estimate diffusion and reaction rates. In FCS the fluorescence coming from a small volume is recorded and the autocorrelation function (ACF) of the fluorescence fluctuations is computed. Scaling out the fluctuations due to the emission process, this ACF can be related to the ACF of the fluctuations in the number of observed fluorescent molecules. In this paper the ACF of the molecule number fluctuations is studied theoretically, with no approximations, for a reaction-diffusion system in which the fluorescence changes with binding and unbinding. Theoretical ACFs are usually derived assuming that fluctuations in the number of molecules of one species are instantaneously uncorrelated to those of the others and obey Poisson statistics. Under these assumptions, the ACF derived in this paper is characterized only by the diffusive timescale of the fluorescent species and its total weight is the inverse of the mean number of observed fluorescent molecules. The theory is then scrutinized in view of previous experimental results which, for a similar system, gave a different total weight and correct estimates of other diffusive timescales. The total weight mismatch is corrected by assuming that the variance of the number of fluorescent molecules depends on the variance of the particle numbers of the other species, as in the variance decomposition formula. Including the finite acquisition time in its computation, it is shown that the ACF depends on various timescales of the system and that its total weight coincides with the one obtained with the variance decomposition formula. This calculation implies that diffusion coefficients of nonobservable species can be estimated with FCS experiments performed in reaction-diffusion systems. Ways to proceed in future experiments are also discussed.

DOI: [10.1103/PhysRevE.102.052407](https://doi.org/10.1103/PhysRevE.102.052407)

### I. INTRODUCTION

The advancement in various biophysical techniques has given the opportunity to observe physiologically relevant processes at the level of one or a few biomolecules. These processes are often characterized by fluctuations, which are usually a complication, but their analysis can give hints on how the processes occur and allow the quantification of biophysical parameters. Fluorescence correlation spectroscopy (FCS) is an optical technique that uses the analysis of fluctuations to quantify transport processes and reaction rates that have been used *in vitro* and *in vivo* in a variety of systems [1–5]. In FCS the fluorescence intensity coming from a relatively small volume ( $\sim 1$  fl) is recorded and the fluctuations about its mean are subsequently analyzed. The statistical analysis of these fluctuations provides a noninvasive way to obtain information about some of the underlying processes that originate them, among them, the diffusion and binding and unbinding reaction rates of the fluorescent molecules. In FCS the autocorrelation function (ACF) of the fluorescence fluctuations is computed from which the correlation times are derived by fitting the ACF with prototypical expressions. When there is a mechanistic model of the underlying processes, some biophysical parameters can be derived from the

correlation times and the weights with which they enter the ACF [6–10].

The aim of the present paper is to determine the timescales that can be derived from the application of FCS to reaction-diffusion systems in which the fluorescence emission changes due to binding and unbinding. This is motivated in that  $\text{Ca}^{2+}$ , an ubiquitous intracellular messenger [11–13], is usually visualized with dyes that change their fluorescence properties upon  $\text{Ca}^{2+}$  binding [14]. Intracellular  $\text{Ca}^{2+}$  signals elicit different cell responses depending on their time and spatial ranges. These ranges not only depend on the rates of cytosolic  $\text{Ca}^{2+}$  entry and *free* diffusion, but also on the interaction of the ions with the various  $\text{Ca}^{2+}$  buffers [15–20], usually proteins that bind to  $\text{Ca}^{2+}$  [21–23] changing the free  $\text{Ca}^{2+}$  concentration and altering its transport properties [24–28]. The expression of endogenous  $\text{Ca}^{2+}$  buffers not only varies from cell to cell but can also change along the lifetime of a cell. The dye itself is a  $\text{Ca}^{2+}$  chelator that modifies the  $\text{Ca}^{2+}$  transport rate. Having reliable estimates of the *free* diffusion coefficients of  $\text{Ca}^{2+}$ , its dyes, and its buffers and of their reaction rates *separately* is then key to go from an intracellular  $\text{Ca}^{2+}$  image to the quantification of the underlying  $\text{Ca}^{2+}$  distribution [29,30] and to derive a comprehensive description of the signals beyond the particular situation probed in each experiment. The theoretical analyses presented in this paper show that FCS experiments allow the estimation of free diffusion coefficients in reaction-diffusion systems.

\*Corresponding author: [cvillarruel@df.uba.ar](mailto:cvillarruel@df.uba.ar)

In this paper the ACF of the fluctuations in the number of fluorescent molecules in an observation volume is studied theoretically for the reaction-diffusion system that describes the dynamics of  $\text{Ca}^{2+}$  in the presence of a single wavelength (SW)  $\text{Ca}^{2+}$  dye and the frequently used  $\text{Ca}^{2+}$  chelator, EGTA. As argued in Ref. [31], the ACF of the molecule number fluctuations corresponds to the mean of the fluorescence fluctuations ACF over several experimental realizations. Thus the correlation times of the molecule number fluctuations are determined by the mean ACF of the fluorescence fluctuations. In spite of its simplicity, the model analyzed here (see Appendix 1 for the five evolution equations that describe it) gives a framework for the interpretation of the experimental results that might be obtained when using FCS in real cells. It is also applicable to the situation probed experimentally in Ref. [32], where FCS experiments were performed in aqueous solutions containing  $\text{Ca}^{2+}$ , the SW  $\text{Ca}^{2+}$  dye Fluo4, and EGTA. In Ref. [32] the experimental results were interpreted using an approximation of the ACF that is valid when the reaction timescales ( $\tau_r$ ) are much smaller than those of diffusion ( $\tau_d$ ). The advantage of this *fast reaction approximation* is that it provides an analytic expression of the ACF [8,33]. Its validity in the case of the experiments of [32], however, is questionable. In particular, the timescale of the reaction between  $\text{Ca}^{2+}$  and the dye is larger than all the diffusion timescales with the exception of the time it takes for one dye molecule to diffuse across the largest axis of the observation volume. Although the studies of [33] showed that the fast reaction approximation gives good estimates of the correlation timescales even for  $\tau_d \lesssim \tau_r$ , it is not clear that this result applies to systems with SW  $\text{Ca}^{2+}$  dyes as those of the experiments in Refs. [32,34]. On the other hand, the best fits to the experiments of [32] corresponded to a two component ACF, while the one prescribed by the fast reaction approximation was much more complicated (see Appendix 2). In spite of this, the diffusion coefficients derived from the fits were approximately equal (within the experimental error) to two of the theoretically expected values of the coefficients of the system for each of the  $\text{Ca}^{2+}$  concentrations probed.

In this work the ACF is studied theoretically for the system of interest without using the fast reaction approximation. Theoretical ACFs are usually computed assuming that fluctuations, at a given time, in the number of molecules of one species in the observation volume are uncorrelated from those of the other species at the same time and that they obey Poisson statistics [31]. Under these usual assumptions on the instantaneous correlations, the studies of the present paper show that the ACF is characterized by only one diffusive timescale: the one that corresponds to the free diffusion coefficient of the fluorescent species (i.e., the  $\text{Ca}^{2+}$ -bound dye, which is assumed to diffuse at the same rate as the free dye). The theory is then reanalyzed in view that other diffusive timescales could be estimated correctly in the experiments of [32]. In particular, the usual assumptions [31] on the instantaneous correlations described before are questioned. In this regard, there are two aspects for consideration. On one hand is the possible existence of correlations between the fluctuations in the number of free and of  $\text{Ca}^{2+}$ -bound dye molecules due to the binding and unbinding reactions with  $\text{Ca}^{2+}$ . On the other hand is how fluctuations in the number

of  $\text{Ca}^{2+}$  ions affect the statistics of the fluctuations in the molecule number of the  $\text{Ca}^{2+}$ -bound dye. These aspects are studied numerically and, the latter, analytically, in the present paper. Using the variance decomposition formula, it is shown that fluctuations in the number of free  $\text{Ca}^{2+}$  ions increase both the variance of the number of  $\text{Ca}^{2+}$ -bound dye molecules and the total weight of the ACF, which solves a disagreement between the theory and the experimental results of [32]. In the experiments, this interspecies variance dependence arises because *instantaneous* actually means during the finite acquisition time. The ACF of the fluctuations in the number of  $\text{Ca}^{2+}$ -bound dye molecules is then computed including this finite time. The expression obtained is the sum of the auto- and cross-correlation functions of the particle number fluctuations of all the species of the system. This implies that the ACF can have components with other timescales besides the one associated to the free diffusion of the dye. In fact, the analysis of the diffusive timescales of the nonfluorescent species that were derived in Ref. [32] shows that they correspond to the components of the free  $\text{Ca}^{2+}$  ions ACF with the largest weight at each  $\text{Ca}^{2+}$  concentration probed. The ability to derive other diffusion coefficients besides the one of the dye is confirmed by the additional experiments performed with another  $\text{Ca}^{2+}$  dye that are presented at the end of the paper. These results lead to the important conclusion that the combination of nonlinearities and of a finite acquisition time allows the transport properties of nonfluorescent species to be estimated with FCS experiments in reaction-diffusion systems.

The organization of the paper is as follows. In Sec. II, a brief description is presented of the usual theory with which FCS experiments are analyzed. In Sec. III, the analysis, without approximations, of the ACF of the fluctuations in the number of fluorescent molecules for the  $\text{Ca}^{2+}$ , dye, EGTA reaction-diffusion system is presented. In Sec. IV the validity of the usual assumptions on the instantaneous correlations and the statistics of the particle number fluctuations of the various species is studied numerically. The second aspect is also studied analytically using the variance decomposition formula to relate the variance of the number of fluorescent molecules with those of the other species. Section IV closes with the analysis of the effect of the finite (experimental) acquisition time on the variance and the ACF. In Sec. V the theoretical results of Sec. IV are used to interpret the experimental results of [32]. Experimental results that validate the main conclusions of the theoretical studies are also presented in Sec. V. Finally the main results and conclusions are summarized in Sec. VI.

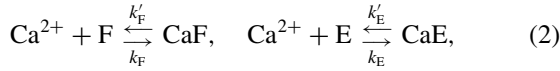
## II. FCS THEORY

In fluorescence correlation spectroscopy (FCS) the fluorescence,  $f(t)$ , coming from a small volume is recorded over time and analyzed. In particular, the time-averaged autocorrelation function (ACF) of the fluorescence fluctuations is computed as

$$G(\tau) = \frac{\langle \delta f(t) \delta f(t + \tau) \rangle}{\langle f(t) \rangle^2}, \quad (1)$$

where  $\langle f(t) \rangle$  is the average fluorescence in the sampling volume and  $\delta f(t)$  is the deviation with respect to this mean at

each time,  $t$ . Fitting the ACF with prototypical expressions the correlation times can be extracted from which, using an underlying mechanistic model, biophysical parameters can be inferred. The case of interest for the present paper is a reaction-diffusion system composed of  $\text{Ca}^{2+}$ , a single wavelength  $\text{Ca}^{2+}$  dye, F, and a  $\text{Ca}^{2+}$  buffer, E. The relevant species are then five: free buffer (E), free dye (F),  $\text{Ca}^{2+}$ -bound buffer (CaE),  $\text{Ca}^{2+}$ -bound dye (CaF), and free  $\text{Ca}^{2+}$ , that diffuse with free coefficients  $D_E$  (E and CaE),  $D_F$  (F and CaF), and  $D_{\text{Ca}^{2+}}$  ( $\text{Ca}^{2+}$ ), and react according to [32]



with on and off rates,  $k_F$ ,  $k_E$  and  $k'_F$ ,  $k'_E$  respectively. The notation,  $C_s$ , will be either used for the concentrations or for the species with the following order:  $C_1 = \text{E}$ ,  $C_2 = \text{F}$ ,  $C_3 = \text{CaE}$ ,  $C_4 = \text{CaF}$ , and  $C_5 = \text{Ca}^{2+}$ . As done in Refs. [32,34] the theoretical calculations are performed under the assumption that CaF is the only fluorescent species and that changes in the number of these molecules inside the observation volume is the main source of fluctuations, i.e., fluctuations due to the emission or detection processes are not included (see, e.g., Ref. [31] for a discussion on this assumption). The stochastic variables of the problem are therefore the numbers of molecules of each species,  $N_i$ , in the observation volume which, as done in Ref. [31], are computed as integrals in the space of the corresponding species concentrations. Thus, for a short enough acquisition time,  $\Delta t$ , the fluorescence as a function of time,  $f(t)$ , can be written as [31]

$$f(t) = \Delta t \int QI(\mathbf{r})[\text{CaF}](\mathbf{r}, t) d^3r, \quad (3)$$

where the parameter,  $Q$ , takes into account the detection efficiency, the fluorescence quantum yield, and the absorption cross section at the wavelength of excitation of the fluorescence and, for experiments performed with confocal microscopy,  $I$  is approximated by a three-dimensional Gaussian:

$$I(\mathbf{r}) = I(0)e^{-\frac{2r^2}{w_r^2}}e^{-\frac{2z^2}{w_z^2}}, \quad (4)$$

with  $w_z$  and  $w_r$  the sizes of the beam waist and  $z$  and  $r$  the spatial coordinates along the beam propagation and the perpendicular directions, respectively. Equation (3) is actually an approximation that assumes that the acquisition time,  $\Delta t$ , is small enough so that there is no need to integrate  $[\text{CaF}](\mathbf{r}, t)$  along the acquisition time interval. This integral will be included later to analyze the implications of the finite acquisition time on the computation of the ACF.

Fluctuations in the number of molecules, or, correspondingly, in their concentrations, are assumed to occur about a mean that is defined by the spatially uniform equilibrium solution,  $[\text{Ca}^{2+}]_{eq}$ ,  $[\text{F}]_{eq}$ ,  $[\text{CaF}]_{eq}$ ,  $[\text{E}]_{eq}$ , and  $[\text{CaE}]_{eq}$ , of Eqs. (A1) which satisfies

$$[\text{CaF}]_{eq} = \frac{[\text{Ca}^{2+}]_{eq}[\text{F}]_{tot}}{[\text{Ca}^{2+}]_{eq} + K_{dF}}, \quad [\text{CaE}]_{eq} = \frac{[\text{Ca}^{2+}]_{eq}[\text{E}]_{tot}}{[\text{Ca}^{2+}]_{eq} + K_{dE}}, \quad (5)$$

where  $K_{dF} = k'_F/k_F$  and  $K_{dE} = k'_E/k_E$  are the dissociation constants of the reactions and  $[\text{F}]_{tot} = [\text{F}]_{eq} + [\text{CaF}]_{eq}$  and  $[\text{E}]_{tot} = [\text{E}]_{eq} + [\text{CaE}]_{eq}$  are the total dye and EGTA concentrations, respectively. Namely, it is assumed that  $\langle N_{\text{Ca}^{2+}} \rangle = \int d^3r I(\mathbf{r})[\text{Ca}^{2+}]_{eq} = V_{ef}[\text{Ca}^{2+}]_{eq}$  with  $V_{ef} = \pi^{3/2}w_r^2w_z$ , the observation volume, and similar expressions for the other species. Thus the ACF is written as

$$G(\tau) = \frac{1}{[\text{CaF}]_{eq}} \int d^3r' \int d^3r I(\mathbf{r})I(\mathbf{r}') \times \langle \delta[\text{CaF}](\mathbf{r}', t + \tau)\delta[\text{CaF}](\mathbf{r}, t) \rangle. \quad (6)$$

Assuming that a linearized version of the model equations [35] provides a correct description of the fluctuations [31], the ACF can be written as a sum of integrals, each one associated to one of the branches of eigenvalues of the linearized system. Given the linearity of the equations, these integrals, which constitute the *components* of the ACF, are usually computed in Fourier space [31] (also see Appendix 3). Therefore, they are integrals over the wave number,  $\mathbf{q}$ , the variable conjugate to the position vector,  $\mathbf{r}$ , in real space. In the case of interest here, there are five branches of eigenvalues,  $\lambda_i(q)$ ,  $i = 1, \dots, 5$ , that, in principle, depend on the norm,  $q \equiv |\mathbf{q}|$ . Two of the branches are purely diffusive, one of them associated to the free diffusion coefficient of the dye,  $D_F$ , and the other to the free diffusion coefficient of the nonfluorescent chelator,  $D_E$ :

$$\lambda_4 = -D_F q^2, \quad (7)$$

$$\lambda_5 = -D_E q^2. \quad (8)$$

This type of eigenvalue leads to ACF components of the form

$$G_i(\tau) = \frac{A_i}{(1 + \frac{\tau}{\tau_f})\sqrt{1 + \frac{\tau}{w^2\tau_f}}}, \quad (9)$$

where  $w = w_z/w_r$  is the aspect ratio of the observation volume and  $\tau_f = w_r^2/(4D_f)$  [with  $D_f = D_F$  in Eq. (7) and  $D_f = D_E$  in Eq. (8)] is the diffusion time across the shortest axis of this volume [5]. Under the usual assumptions on the instantaneous correlations [31] (also see Sec. IV) it is  $A_5 = 0$  and  $A_4 = 1/[\text{F}]_{tot}V_{ef}$ . The other branches are more complicated but, for small enough  $q$ , can be approximated by

$$\lambda_i \approx \lambda_{efi} \equiv -\nu_{efi} - D_{efi}q^2, \quad i = 1, 2, 3. \quad (10)$$

If this approximation holds throughout the range of  $q$  values that contribute non-negligibly to the corresponding ACF component,  $G_i(\tau)$ , then  $G_i(\tau)$  can be approximated by

$$G_i(\tau) \approx \frac{A_i e^{-\nu_{efi}\tau}}{(1 + \frac{\tau}{\tau_i})\sqrt{1 + \frac{\tau}{w^2\tau_i}}}. \quad (11)$$

This approximation is valid in the *fast reaction* limit (see Appendix 2). In the opposite *fast diffusion* limit the components are either purely diffusive [as in Eq. (11) with  $\nu_{efi} = 0$ ] or purely exponential [as in Eq. (11) with  $\tau_i \rightarrow \infty$ ] [36]. As in Eq. (11), the notation  $A_i$  will be used throughout the paper to denote the weight of the  $i$ th component, i.e.,  $A_i \equiv G_i(\tau = 0)$ .

TABLE I. Model parameters used to generate theoretical figures. The values of  $[\text{Ca}^{2+}]_{\text{tot}}$  are described in each figure. Lengths are in  $\mu\text{m}$ , time in s, and concentrations and dissociation constants in  $\mu\text{M}$ , when not explicitly mentioned.

	Concentration	$D$	$K_d$	$k'$
$\text{Ca}^{2+}$	(9.27–10.4) mM	$D_{\text{Ca}^{2+}} = 760$		
EGTA	$[\text{E}]_{\text{tot}} = 9.66$ mM	$D_E = 405/352$	$K_{dE} = 0.15$	$k'_E = 0.75$
Fluo4	$[\text{F}]_{\text{tot}} = 0.676$	$D_F = 85$	$K_{dF} = 2.6$	$k'_F = 300$
Fluo8	$[\text{F}]_{\text{tot}} = 0.676$	$D_F = 100$	$K_{dF} = 0.432$	$k'_F = 47.5$
Microscopy parameters				
	$w_r = 0.28$ $\mu\text{m}$ ,	$w = 5$		

Regardless of whether there are analytic expressions for the nontrivial components, under the usual assumptions on the instantaneous correlations, the total weight of the ACF is

$$G_{\text{tot}} \equiv G(\tau = 0) = \frac{\text{Var}(N_{\text{CaF}})}{\langle N_{\text{CaF}} \rangle^2} = \frac{1}{V_{\text{eff}}[\text{CaF}]_{\text{eq}}}. \quad (12)$$

### III. COMPLETE ANALYSIS OF THE EIGENVALUES AND OF THE ACF FOR THE REACTION-DIFFUSION SYSTEM WITH $\text{Ca}^{2+}$ , DYE, AND EGTA

In this section the nontrivial eigenvalue branches of Eqs. (A1) linearized around equilibrium and the weights with which they contribute to the ACF are analyzed without taking the fast diffusion or fast reaction limits. The weight computation is done under the usual assumptions on the initial correlations, performing the integrals as explained in the Appendix 4. For all computations we use the parameter values of Table I considering that the dye is Fluo4 and  $D_E = 405 \mu\text{m}^2$ . The range of total concentration values embraces those used in the experiments of [32].

#### A. Branches of eigenvalues, diffusion coefficients, and component weights

Figure 1 shows the exact nontrivial eigenvalue branches,  $\lambda_i$  ( $i = 1, 2, 3$ ) ( $\lambda_1 > \lambda_2 > \lambda_3$ ), as functions of  $q^2$  for three representative cases ( $[\text{Ca}^{2+}]_{\text{tot}} = 9.3, 9.6,$  and  $10.4$  mM) of

those explored experimentally in Ref. [32]. The three approximated eigenvalues,  $\lambda_{efi}$ , that are obtained by expanding each  $\lambda_i$  around  $q = 0$  and keeping terms up to  $O(q^2)$  are also plotted. These approximated eigenvalues are of the form Eq. (10) with  $D_{efi}$  the effective coefficients and  $v_{efi}$  the effective rates of the fast reaction approximation derived in Ref. [32]. Figure 2(a) shows the three effective and the three free diffusion coefficients of the problem and Fig. 2(b) shows the rates  $v_{ef2}$  and  $v_{ef3}$ , in all cases, as functions of  $[\text{Ca}^{2+}]_{\text{tot}}$  within the range of concentration values studied experimentally in Ref. [32]. It can be observed in Fig. 2(a) that both for small and large  $[\text{Ca}^{2+}]_{\text{tot}}$  each of the effective diffusion coefficients is approximately equal to a free diffusion one, but not the same at both ends. Figure 1 shows that each  $\lambda_i(q^2)$  behaves as a piecewise linear function of  $q^2$  for most values of  $q$ . This implies that expressions of the form of Eq. (10) give a good approximation of each branch of nontrivial eigenvalues but with slopes and, therefore, diffusion coefficients, that are different depending on the range of  $q$  values. The slope of each of these functions is  $-D_{efi}$  for  $q \approx 0$  and  $-D_i$ , with  $D_i$  one of the free diffusion coefficients of the problem,  $D_F$ ,  $D_E$ , or  $D_{\text{Ca}^{2+}}$ , for  $q$  large enough, but  $D_i$  is not necessarily similar to  $D_{efi}$  for each  $i$ . This means that each eigenvalue can be associated to a different diffusion coefficient depending on the wave number,  $q$ . The exponential rates, which also vary with  $q^2$ , are most relevant for  $q \approx 0$  for which they coincide with the values prescribed by the fast reaction approximation.

Figure 2(c) shows the weights of each of the four components of the ACF and their sum [i.e., the total weight,  $G_{\text{tot}} = G(\tau = 0)$ ], as functions of  $[\text{Ca}^{2+}]_{\text{tot}}$ , computed as explained in the Appendix 4. It can be observed that the weight,  $A_4$ , associated to the free diffusion coefficient of the dye is the largest in all cases. Furthermore, we observe that, at least up to  $[\text{Ca}^{2+}] \sim 9.7$  mM, the weights  $A_2$  and  $A_3$  are negligible with respect to the other two. This is consistent with the fact that the best fits of the experimental ACF [32] were obtained using two components, one of which always corresponded to the timescale associated to the free diffusion coefficient of the dye,  $D_F$ . As may be observed in Fig. 2(c), up to  $[\text{Ca}^{2+}]_{\text{tot}} \sim 9.85$  mM, the second largest weight is  $A_1$ , the one associated to  $\lambda_1$ . For this range of  $[\text{Ca}^{2+}]_{\text{tot}}$  values

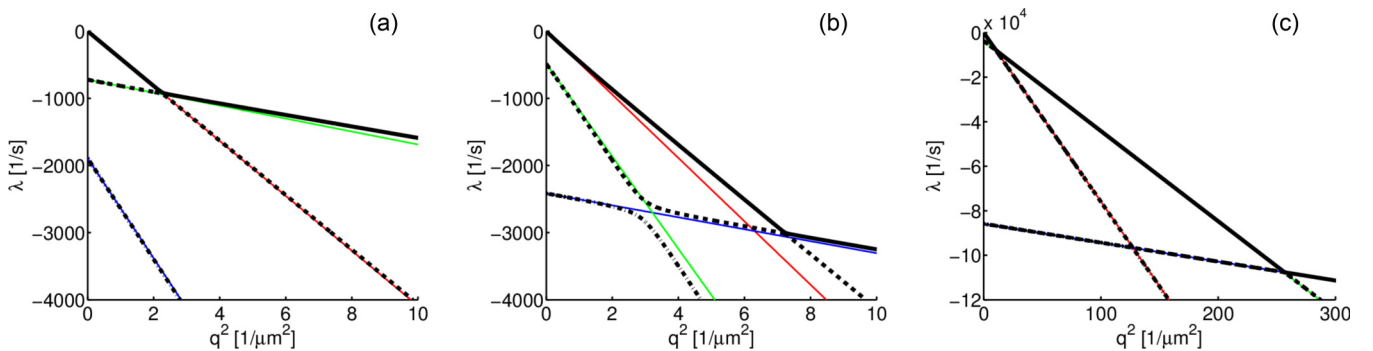


FIG. 1. Three nontrivial eigenvalue branches as functions of the squared wave number,  $q^2$ , of the linearized reaction-diffusion equations that correspond to a system with  $\text{Ca}^{2+}$ , dye, and Fluo4 with the corresponding parameters of Table I,  $D_E = 405 \mu\text{m}^2/\text{s}$  and the total  $\text{Ca}^{2+}$  concentrations:  $[\text{Ca}^{2+}]_{\text{tot}} = 9300 \mu\text{M}$  in (a),  $[\text{Ca}^{2+}]_{\text{tot}} = 9600 \mu\text{M}$  in (b), and  $[\text{Ca}^{2+}]_{\text{tot}} = 10400 \mu\text{M}$  in (c). In the three subfigures  $\lambda_1$  is shown with solid lines,  $\lambda_2$  with dashed lines, and  $\lambda_3$  with dashed-dotted lines. The effective eigenvalues,  $\lambda_{ef1}$ ,  $\lambda_{ef2}$ , and  $\lambda_{ef3}$ , are also plotted with thin blue solid lines.

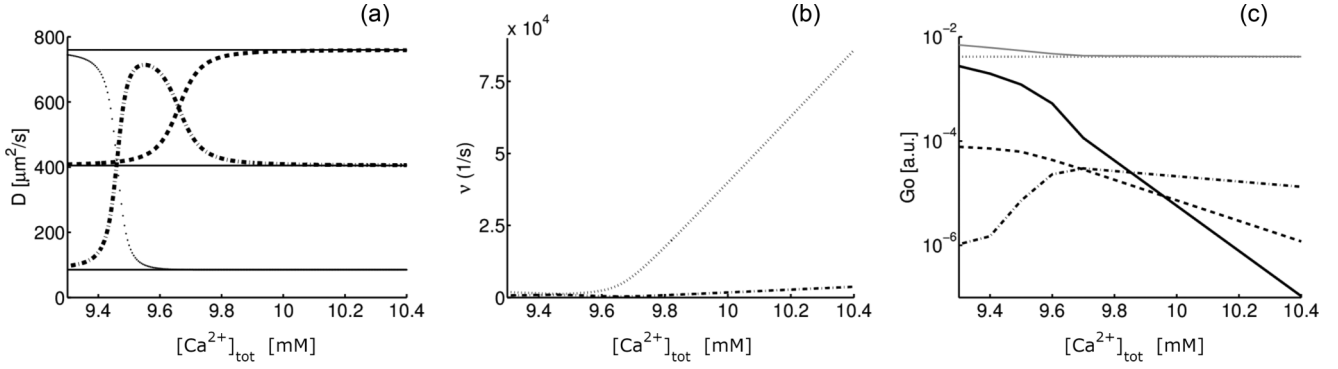


FIG. 2. (a) Effective ( $D_{ef1}$ : dashed line;  $D_{ef2}$ : dotted line;  $D_{ef3}$ : dashed-dotted line) and free (solid lines,  $D_{Ca^{2+}} > D_E > D_F$ ) diffusion coefficients as functions of  $[Ca^{2+}]_{tot}$  computed for a reaction-diffusion system with  $Ca^{2+}$ , EGTA, and Fluo4 and the corresponding parameters of Table I with  $D_E = 405 \mu m^2/s$ . (b) Similar to (a) but for the effective rates  $v_{ef2}$  (dotted line) and  $v_{ef3}$  (dashed-dotted line). (c) Similar to (a) but for the total weight ( $G_{tot}$ : gray solid line) and the weights of the four components of the ACF ( $A_1$ : solid line;  $A_2$ : dashed line;  $A_3$ : dashed-dotted line;  $A_4$ : dotted line).

Fig. 1(a) shows that  $\lambda_1 \sim -D_{ef1}q^2$  and that  $D_{ef1} \approx D_E$  in Fig. 2(a). For this range of concentrations, the correlation time derived from the experiments of [32] that did not correspond to the free diffusion of the dye,  $D_F$ , corresponded to the diffusion coefficient,  $D_E$ . Different from what Fig. 2(c) shows, however, the experimental fit gave the largest weight for this timescale.

For the intermediate  $[Ca^{2+}]_{tot}$  values explored in Ref. [32] ( $[Ca^{2+}]_{tot} \sim 9.47-9.66$  mM) the second largest weight according to Fig. 2(c) is  $A_1$ . The corresponding eigenvalue satisfies  $\lambda_1 \approx -D_{ef1}q^2$  for  $q \approx 0$ . As shown in Fig. 2(a), for the intermediate range of concentrations,  $D_{ef1}$  is noticeably smaller than the coefficient,  $D_{ef2}$ , that could be derived experimentally, besides  $D_F$ , in Ref. [32].

Finally, the case of the largest  $[Ca^{2+}]_{tot}$  values explored in Ref. [32] ( $[Ca^{2+}]_{tot} \sim 10$  mM) is analyzed. For this range of concentrations, the second timescale obtained with the fitting of the experiments seemed to correspond again to  $D_{ef2}$  which, in this range, is approximately equal to the intermediate free coefficient of the problem,  $D_{ef2} \approx D_E$  [Fig. 2(a)]. In this case the nontrivial component with the largest weight is the one corresponding to  $\lambda_3$  [see Fig. 2(b)]. This eigenvalue is  $\lambda_3 \approx -v_{ef3} - D_F q^2$  up to  $q^2 \sim 125 \mu m^2$ . Thus the diffusionlike decay of this component is pretty much dominated by  $D_F$  and it would be impossible to separate it from the term associated to  $\lambda_4 = -D_F q^2$ ,  $G_4$ . Furthermore, the fact that  $v_{ef3} \sim 85000$  s for this range of  $[Ca^{2+}]_{tot}$  values [see Fig. 2(b)] while  $\tau_{DF} \sim w_r^2/(4D_F) \sim 2.3 \times 10^{-4}$  s means that the contribution of this component to the sum  $G_4 + G_3$  will be small at least at the correlation time  $\tau_{DF}$ .

The analysis performed so far shows that the ACF component with the largest weight is the one characterized by the free diffusion coefficient of the dye,  $D_F$ , for all the  $Ca^{2+}$  concentrations probed. The other eigenvalues are characterized by more than one diffusion timescale depending on the wave number (see Fig. 1). The timescale that might eventually be derived from a fitting would then depend on the relative weight with which the different wave numbers contribute to the corresponding component of the ACF. This aspect is studied in what follows.

## B. Weight densities

In this section the functions,  $g_i(q, \varphi)$ , that give the total weight of each component,  $A_i$ , when integrated over  $q$  and the angle,  $\varphi$ , that the wave number vector,  $\mathbf{q}$ , forms with the plane perpendicular to the optical axis,  $z$ , is analyzed. The functions,  $g_i(q, \varphi)$ , are weight densities that satisfy

$$A_i = \int_0^\infty dq \int_0^\pi d\varphi g_i(q, \varphi). \quad (13)$$

Figures 3(a)–3(c) show plots of  $g_i(q, \varphi)$ ,  $i = 1, 2, 3$ , for  $\varphi = \pi/2$  and the same  $[Ca^{2+}]_{tot}$  values of Fig. 1 [ $\varphi = \pi/2$  was chosen because it is the angle at which the functions,  $g_i(q, \varphi)$ , attain their maximum values]. Figure 3(d) shows the density,  $g_{oF}$ , that corresponds to the eigenvalue,  $\lambda_4$ , associated to the free diffusion of the dye [see Eq. (7)] for the case with  $[Ca^{2+}]_{tot} = 10.4$  mM. This density is of the form  $g_i(q, \pi/2) = \alpha q^2 \exp(-q^2 w_r^2/4)$  with constant  $\alpha$  for any value of  $[Ca^{2+}]_{tot}$  as is the case for any eigenvalue of the form Eq. (10) with fixed values,  $v_{efi}$ ,  $D_{efi}$ , for all  $q$ . In Figs. 3(a)–3(c) it can be observed that this is not the case for any of the nontrivial eigenvalues. However, the best fits of the experimental data of [32] were obtained with two purely diffusive components (i.e.,  $\lambda_i = -D_i q^2$ ), one of which always corresponded to the free diffusion coefficient of the dye,  $D_F$  [the component with the largest weight according to the results of Fig. 2(c)]. Figure 3 shows that the values of the weight densities,  $g_i(q, \pi/2)$ ,  $i = 1, 2, 3$ , alternate in the sense that the range of  $q^2$  over which one of them is largest the other two are almost negligible. If Figs. 3(a)–3(c) are compared with Figs. 1(a)–1(c), respectively, it can be observed that the range of wave numbers,  $q$ , for which each weight density,  $g_i(q, \pi/2)$ ,  $i = 1, 2, 3$ , is largest [e.g.,  $g_3$  for  $q^2 < 3 \mu m^2$ ,  $g_2$  for  $3 \mu m^2 < q^2 < 7.3 \mu m^2$ , and  $g_1$  for  $q^2 > 7.3 \mu m^2$  in Fig. 3(b)], the corresponding eigenvalue,  $\lambda_i$  [ $\lambda_3$  for  $q^2 < 3 \mu m^2$ ,  $\lambda_2$  for  $3 \mu m^2 < q^2 < 7.3 \mu m^2$ , and  $\lambda_1$  for  $q^2 > 7.3 \mu m^2$  in Fig. 1(b)] is such that  $\lambda_i = -D_F q^2 - v_{ef}$  with the same  $v_{ef}$  in all cases. Furthermore, by looking at the  $q^2$  dependence of the largest weight density in each case we conclude that, if we only keep the largest  $g_i(q, \pi/2)$ ,  $i = 1, 2, 3$ , for all  $q^2$ , we are left with a weight density as

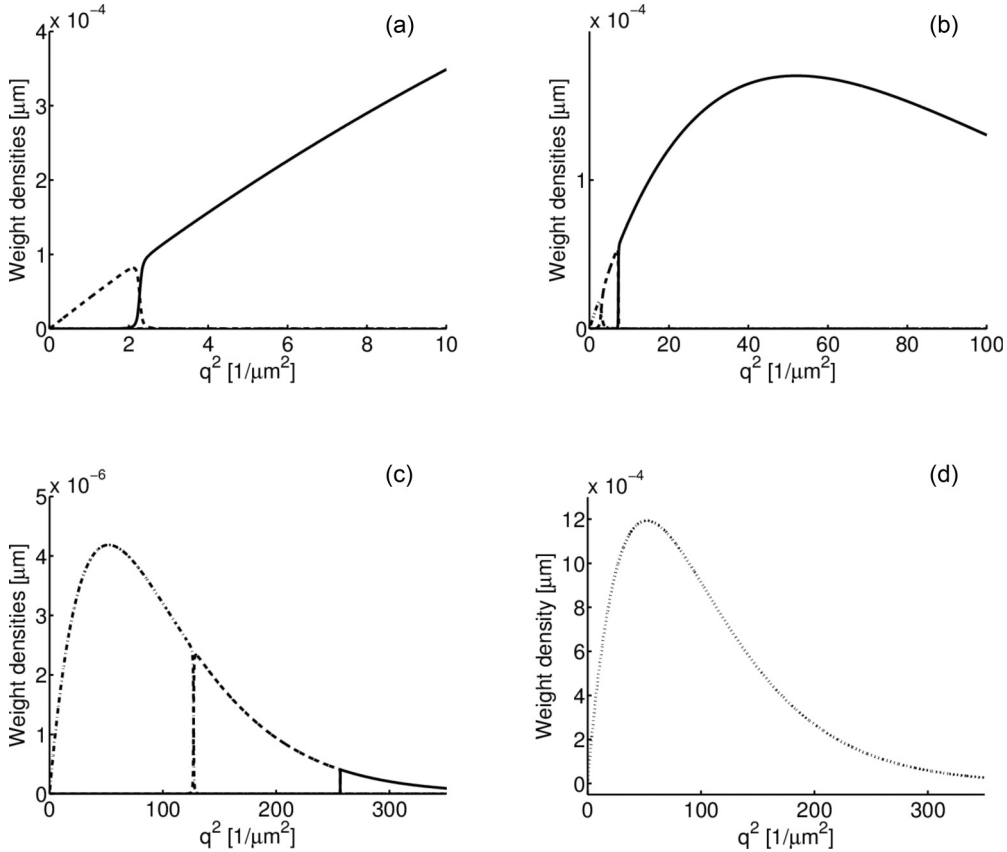


FIG. 3. Weight densities,  $g_i(q, \varphi = \pi/2)$ , as functions of the squared wave number,  $q^2$ . The ones that correspond to the three branches of nontrivial eigenvalues of Fig. 1 are shown in (a)–(c) for the same  $\text{Ca}^{2+}$  concentrations and symbols as in Fig. 1. The density that corresponds to  $\lambda_4$ , the eigenvalue associated to the free diffusion coefficient of the dye, is shown in (d) for the case with  $[\text{Ca}^{2+}]_{\text{tot}} = 10.4 \text{ mM}$ .

the one in Fig. 2(d) [e.g., compare Figs. 2(c) and 2(d)]. In this way, when integrated over  $q^2$ , the sum of the weights of the nontrivial eigenvalues leads to a component of the form of Eq. (11) with the diffusive timescale,  $\tau_i$ , given by the free diffusion coefficient of the dye.

The analysis of the weight densities shows that the ACF should be characterized by only one diffusive timescale, the one associated to  $D_F$ . Why have other diffusive timescales been estimated correctly in the experiments of [32]?

#### IV. WHAT FLUCTUATIONS ARE MEASURED WITH FCS EXPERIMENTS THAT USE SINGLE-WAVELENGTH $\text{Ca}^{2+}$ DYES?

##### A. Instantaneous fluctuations and resulting ACF

Computing the ACF [Eq. (6)] as done in Ref. [31] requires knowledge of how fluctuations in the concentration of fluorescent molecules,  $\delta[\text{CaF}]$ , at a certain time,  $t + \tau$ , and position within the observation volume,  $\mathbf{r}'$ , are related to the fluctuations at a previous time,  $t$ , and any other position,  $\mathbf{r}$ , in the volume. The resulting ACF then depends on the correlations between  $\delta[\text{CaF}](\mathbf{r}', t)$  and fluctuations in all the species concentrations,  $\delta C_s(\mathbf{r}, t)$ ,  $s = 1, \dots, 5$ , at the same time,  $t$  [31]:

$$\langle \delta[\text{CaF}](\mathbf{r}, t) \delta C_s(\mathbf{r}', t) \rangle. \quad (14)$$

It is usually assumed [31] that fluctuations in the concentrations of different species are instantaneously uncorrelated, that they obey Poisson statistics [i.e., that the variance and the mean of the number of molecules of each species,  $N_i$ , in the observation volume,  $V_{ef}$ , satisfy  $\text{Var}(N_i) = \langle N_i \rangle$ ], and that correlations are spatially short ranged so that [31]

$$\langle \delta C_s(\mathbf{r}, t) \delta C_{s'}(\mathbf{r}', t) \rangle = \delta_{ss'} \delta(\mathbf{r} - \mathbf{r}') C_{s,eq}, \quad (15)$$

where  $C_{s,eq}$  is the equilibrium concentration of the  $s$ th species. Given the linearity of the equations with which the dependence of  $\delta[\text{CaF}](\mathbf{r}', t + \tau)$  on  $\delta C_s(\mathbf{r}, t)$ ,  $s = 1, \dots, 5$ , is computed, each eigenvalue and eigenvector (with their corresponding timescales) evolves separately. The “initial” (actually, instantaneous) correlations of Eq. (14) then determine the weight with which each of these eigenmodes (with their corresponding timescales) contribute to the ACF. The relative weights of the various modes derived in the previous sections are a direct consequence of Eq. (15). It is under this assumption that the total weight of the ACF in the case of a single fluorescent species,  $C_4 = \text{CaF}$ , is given by Eq. (12) and that the ACF has four, rather than five, components that, when added together, are characterized by a single diffusive timescale,  $\tau_F$ , as shown in Sec. III B.

Fluctuations in the concentrations of  $\text{Ca}^{2+}$ -bound and free dye molecules can be instantaneously correlated depending on the origin of the fluctuations. Namely, when a binding reaction occurs creating a  $\text{Ca}^{2+}$ -bound dye molecule, a free

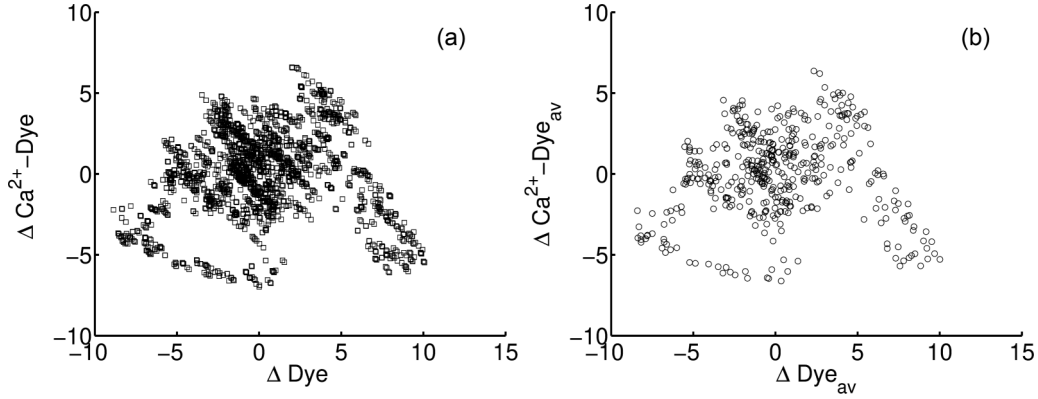


FIG. 4. Stochastic simulations of the reaction-diffusion system of  $\text{Ca}^{2+}$ , dye, and EGTA. Deviation from the mean of the number of  $\text{Ca}^{2+}$ -bound dye molecules as a function of the deviation in the number of free dye molecules in the observation volume. (a) All the data points and (b) average over the observation time interval.

dye molecule is destroyed at the same time and vice versa [see Eq. (2)]. In particular, if the dye were immobile this would imply a complete dependence between the two stochastic variables,  $N_F$  and  $N_{\text{CaF}}$ , which would have a binomial distribution. Some correlation still persists even if the dye diffuses, as we analyzed in Ref. [36]. This (anti)correlation tends to reduce the total weight of the ACF and although it is not what was observed in the experiments of [32] it could explain the fact that the weight of the component associated to the free diffusion coefficient of the dye was not the largest one derived from the fittings. Figure 4 shows the result of stochastic simulations of the reaction-diffusion system of  $\text{Ca}^{2+}$ , dye, and EGTA performed as explained in the Appendix 7. This figure shows the deviation from the mean of the number of  $\text{Ca}^{2+}$ -bound dye molecules as a function of the deviation in the number of free dye molecules in the observation volume, where the contribution of each molecule has been weighted with a Gaussian function of the distance to the center (see Appendix 7 for more details). Figure 4(a) displays all the data points derived from the simulation ( $dt \approx 2 \mu\text{s}$ ) and Fig. 4(b) the numbers averaged over the observation time interval ( $dt_{\text{obs}} = 20 \mu\text{s}$ ). Although some anticorrelation is apparent over a few time steps, fitting the cloud of points did not give any linear correlation. It is possible to conclude that the effect of the anticorrelation in the fluctuations of the number of  $\text{Ca}^{2+}$ -bound dye and of free dye molecules is negligible.

### B. Variance of the number of molecules

The assumption that the ACF is only due to fluctuations in the number of fluorescent particles ( $N_{\text{CaF}}$ ) implies that the total weight of the ACF is the ratio between the variance and the squared mean of  $N_{\text{CaF}}$  [see Eq. (12)]. The dynamics of the total dye,  $F_T$ , or buffer,  $E_T$ , concentrations are purely diffusive. Thus, given that the observation volume  $V_{ef}$  constitutes a small portion of the whole space over which the particles diffuse, the total numbers of dye or EGTA molecules in  $V_{ef}$  are Poisson distributed [37]. Regarding the number of  $\text{Ca}^{2+}$ -bound dye molecules,  $N_{\text{CaF}}$ , if the total number of dye molecules in  $V_{ef}$ ,  $N_{FT}$ , is known and the probability that a dye molecule has  $\text{Ca}^{2+}$  bound,  $p_b$ , is fixed, then  $N_{\text{CaF}}$  (and  $N_F \equiv$

$N_{FT} - N_{\text{CaF}}$ ) would be binomial [ $B(p_b, N_{FT})$ ]. Now, since  $N_{FT}$  is Poisson distributed, then  $N_{\text{CaF}}$  and  $N_F$  would also be Poisson, provided that  $p_b$  is constant. In such a case, the total weight of the ACF would satisfy Eq. (12). However,  $p_b$  is not fixed: it actually fluctuates with the number of  $\text{Ca}^{2+}$  ions,  $N_{\text{Ca}^{2+}}$ , that are in  $V_{ef}$ , which is another stochastic variable. This is apparent considering that  $\langle p_b \rangle = [\text{CaF}]_{eq}/[\text{F}]_{tot}$ , where  $[\text{F}]_{tot}$  is the equilibrium (spatially uniform) total dye concentration. Therefore,  $p_b$ , as a stochastic variable could then be written as

$$p_b = \frac{N_{\text{Ca}^{2+}}}{N_{\text{Ca}^{2+}} + K_{dF}V_{ef}}. \quad (16)$$

It is expected that a fluctuating  $p_b$  should enlarge the variance of  $N_{\text{CaF}}$  with respect to the case with fixed  $p_b$ . We performed stochastic simulations to check whether this could be the case. Figure 5 shows the cumulative distribution function of the  $\text{Ca}^{2+}$ -bound dye molecules in the observation volume obtained with the stochastic simulation of the full reaction-diffusion system (solid line) and when the probability of binding is assumed to be fixed at  $p_b = [\text{Ca}^{2+}]/([\text{Ca}^{2+}] + K_{dF})$  (dashed line).

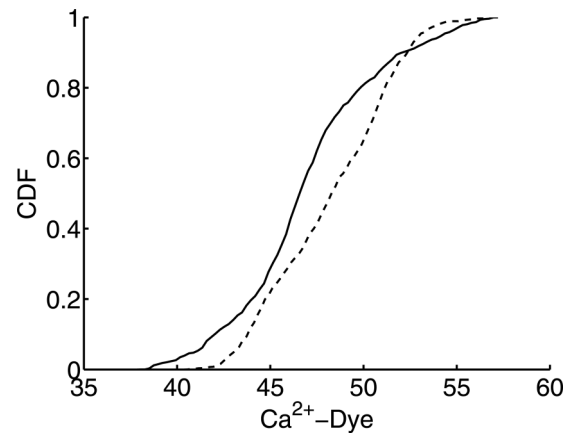


FIG. 5. Cumulative distribution function (CDF) of the  $\text{Ca}^{2+}$ -bound dye molecules in the observation volume obtained with the stochastic simulation of the full reaction-diffusion system (solid line) and when the probability of binding is assumed to be fixed at  $p_b = [\text{Ca}^{2+}]/([\text{Ca}^{2+}] + K_{dF})$  (dashed line).

binding is assumed to be fixed at  $p_b = [\text{Ca}^{2+}]/([\text{Ca}^{2+}] + K_{dF})$  (dashed line). It is apparent that the distributions differ. A Kolmogorov-Smirnov test comparing both data sets rejects the hypothesis that they both come from the same distribution. The variance in the case of the simulations of the full reaction-diffusion system is larger than when a fixed  $p_b$  is used.

The variance decomposition formula is now used to analyze the effect of a fluctuating  $p_b$  on the variance of the  $\text{Ca}^{2+}$ -bound dye molecules in the observation volume. Considering the conditional probability  $P(N_{\text{CaF}} | N_{\text{Ca}^{2+}}, N_{\text{FT}})$  that  $N_{\text{CaF}}$  takes a certain value given that  $N_{\text{Ca}^{2+}}$  and  $N_{\text{FT}}$  take some other values and assuming that  $N_{\text{Ca}^{2+}}$  and  $N_{\text{FT}}$  are independent we obtain (see Appendix 5)

$$\begin{aligned} \text{Var}(N_{\text{CaF}}) &= \langle \text{Var}(N_{\text{CaF}} | N_{\text{Ca}^{2+}}) \rangle_{N_{\text{Ca}^{2+}}} \\ &+ \text{Var}_{N_{\text{Ca}^{2+}}}(\langle N_{\text{CaF}} | N_{\text{Ca}^{2+}} \rangle), \end{aligned} \quad (17)$$

where the two terms are given by Eqs. (A14). As discussed in Sec. V, the assumption that  $N_{\text{Ca}^{2+}}$  and  $N_{\text{FT}}$  are independent holds for the parameters of Table I and the experiments of [32]. Possible further corrections would be to consider the variance decomposition formula for  $N_{\text{Ca}^{2+}}$  making it dependent of  $N_E$ . This is discussed in Sec. IV C.

An exact calculation of the terms in Eq. (17) is not simple so that we approximate them by

$$\begin{aligned} \text{Var}(N_{\text{CaF}}) &= \text{Var}(N_{\text{CaF}})_{|(p_b)} + \left( \frac{dp_b}{dN_{\text{Ca}^{2+}}} \langle N_{\text{FT}} \rangle \right)^2 \text{Var}(N_{\text{Ca}^{2+}}) \\ &= \langle p_b \rangle \langle N_{\text{FT}} \rangle + \left( \frac{dp_b}{dN_{\text{Ca}^{2+}}} \langle N_{\text{FT}} \rangle \right)^2 \text{Var}(N_{\text{Ca}^{2+}}) \\ &= \langle N_{\text{CaF}} \rangle + \alpha \langle N_{\text{Ca}^{2+}} \rangle, \end{aligned} \quad (18)$$

with  $\alpha > 0$ . Using Eq. (18) the total weight of the ACF in Eq. (30) becomes

$$G(0) = \frac{[\text{CaF}]_{eq} V_{ef} + \alpha [\text{Ca}^{2+}]_{eq} V_{ef}}{([\text{CaF}]_{eq} V_{ef})^2}, \quad (19)$$

instead of Eq. (12). Given that  $\alpha > 0$ , under this theory it is  $G(0) > 1/([\text{CaF}]_{eq} V_{ef})$ . Therefore, if the weight derived from the experiments satisfies Eq. (19) and the  $\text{Ca}^{2+}$ -bound dye concentration is derived assuming that  $[\text{CaF}]_{eq} V_{ef} = 1/G(0)$ , a smaller value,  $[\text{CaF}]_{eq}$ , than the actual one would be obtained, exactly as it happens in the experiments of [32].

### C. Finite acquisition time and timescales of the ACF

The conditional variance expression is highlighting that the *instantaneous* fluctuations in  $N_{\text{CaF}}$  depend on those of  $N_{\text{Ca}^{2+}}$ . Here *instantaneous* actually means within the acquisition time. It is implicit in the assumption that the variance of  $N_{\text{CaF}}$  can be written in terms of the instantaneous value of  $N_{\text{Ca}^{2+}}$  and then averaged over all possible values of  $N_{\text{Ca}^{2+}}$  [see Eq. (17)] that there is “enough time” for the free and dye-bound  $\text{Ca}^{2+}$  ions to reach some “local” equilibrium deter-

mined by the current (instantaneous) values of  $N_{\text{FT}}$  and  $N_{\text{Ca}^{2+}}$ . It is implicit in Eq. (3) that the acquisition time,  $\Delta t$ , is very small. Considering its finiteness, Eq. (3) should be rewritten as

$$\delta \bar{f}(n\Delta t) = \int d^3 r Q I(\mathbf{r}) \int_0^{\Delta t} dt_o \delta C_4(\mathbf{r}, n\Delta t + t_o), \quad (20)$$

where  $C_4 = [\text{CaF}]$  as defined before and  $\bar{f}$  denotes the fluorescence collected during the finite acquisition time. The ACF should then be written as

$$\begin{aligned} \langle \delta \bar{f}(n\Delta t) \delta \bar{f}(0) \rangle &= \int d^3 r \int d^3 r' Q^2 I(\mathbf{r}) I(\mathbf{r}') \int_0^{\Delta t} dt_o \\ &\times \int_0^{\Delta t} dt'_o \langle \delta C_4(\mathbf{r}, n\Delta t + t_o) \delta C_4(\mathbf{r}', t'_o) \rangle. \end{aligned} \quad (21)$$

As already explained,  $\delta C_4(\mathbf{r}, t)$  is determined solving the linearized reaction-diffusion system in Fourier space as done in Ref. [31]. This means that it is written as

$$\delta C_\ell(\mathbf{q}, t) = \frac{1}{(2\pi)^{3/2}} \int d^3 r e^{i\mathbf{q}\cdot\mathbf{r}} \delta C_\ell(\mathbf{r}, t) \quad (22)$$

and is given by

$$\delta C_\ell(\mathbf{q}, t) = \sum_{s,k} e^{\lambda_s(\mathbf{q})t} X_{\ell s}(\mathbf{q}) X_{sk}^{-1}(\mathbf{q}) \delta C_k(\mathbf{q}, 0), \quad (23)$$

with  $\lambda_s$  the eigenvalue branches of Sec. III and  $X_{\ell s} = \sum_k B_{\ell k} M_{ks}$ , with  $B$  and  $M$  defined in Eq. (A7). For the sake of simplicity, let us assume for now that there is no diffusion so that neither the eigenvalues nor the eigenvectors depend on the wave number,  $q$ . In such a case it is

$$\begin{aligned} \delta \bar{N}_{\text{CaF}}(0) &= \frac{1}{\Delta t} \int d^3 r I(\mathbf{r}) \int_0^{\Delta t} dt_o \delta C_4(\mathbf{r}, t_o) \\ &= \frac{1}{\Delta t} \int d^3 r I(\mathbf{r}) \int_0^{\Delta t} dt_o \sum_{s,k} e^{\lambda_s t_o} X_{4s} X_{sk}^{-1} \delta C_k(\mathbf{r}, t_o) \\ &= \frac{1}{\Delta t} \int d^3 r I(\mathbf{r}) \sum_{s,k} \frac{e^{\lambda_s \Delta t} - 1}{\lambda_s} X_{4s} X_{sk}^{-1} \delta C_k(\mathbf{r}, 0), \end{aligned} \quad (24)$$

where  $\bar{N}_{\text{CaF}}$  is used to denote that we are considering the time average over the acquisition time. If  $|\lambda_s \Delta t| \ll 1 \forall s$  then Eq. (24) reduces to

$$\begin{aligned} \delta \bar{N}_{\text{CaF}}(0) &\approx \int d^3 r I(\mathbf{r}) \sum_{s,k} X_{4s} X_{sk}^{-1} \delta C_k(\mathbf{r}, 0) \\ &= \int d^3 r I(\mathbf{r}) \delta C_4(\mathbf{r}, 0), \end{aligned} \quad (25)$$

which leads to the same expression of the instantaneous fluorescence fluctuation as the one derived from Eq. (3). Using Eq. (24) we obtain

$$\langle \delta \bar{N}_{\text{CaF}}(0) \delta \bar{N}_{\text{CaF}}(0) \rangle = \frac{1}{\Delta t^2} \int d^3 r I(\mathbf{r}) \int d^3 r' I(\mathbf{r}') \left( \sum_{s,k,\ell,j} \frac{e^{\lambda_s \Delta t} - 1}{\lambda_s} \frac{e^{\lambda_\ell \Delta t} - 1}{\lambda_\ell} X_{4s} X_{sk}^{-1} X_{4\ell} X_{\ell j}^{-1} \langle \delta C_k(\mathbf{r}, 0) \delta C_j(\mathbf{r}', 0) \rangle \right). \quad (26)$$



Thus, considering, as usual, that the actual instantaneous fluctuations satisfy  $\langle \delta C_k(\mathbf{r}, 0) \delta C_j(\mathbf{r}', 0) \rangle = \delta_{kj} C_{k,eq} \delta(\mathbf{r} - \mathbf{r}')$ , the variance of the number of fluorescence molecules (which determines the total weight of the ACF) reads

$$\langle \delta \bar{N}_{CaF}(0) \delta \bar{N}_{CaF}(0) \rangle = \frac{V_{ef}}{\Delta t^2} \sum_k \left[ C_{k,eq} \sum_s \left( \frac{e^{\lambda_s \Delta t} - 1}{\lambda_s} X_{4s} X_{sk}^{-1} \right)^2 \right] \approx V_{ef} C_{4,eq} + V_{ef} \sum_k \left[ C_{k,eq} \sum_s \left( \frac{\lambda_s \Delta t}{2} X_{4s} X_{sk}^{-1} \right)^2 \right], \quad (27)$$

where  $V_{ef} = \int d^3 r I(\mathbf{r})$ . The last approximation in Eq. (27) corresponds to expanding the exponential up to second order in  $\lambda_s \Delta t$ . It shows that, under the usual assumptions on the instantaneous correlations, the variance of the number of fluorescence molecules averaged over the acquisition time is a weighted sum of the variances of all the species. This expression is a generalization of the one we obtained using the variance decomposition formula and assuming that  $N_{Ca^{2+}}$  was Poissonian. Namely neglecting some of the terms in Eq. (27) we obtain an expression of the form of Eq. (18).

A similar calculation can be done to compute the ACF. We write

$$\delta \bar{N}_{CaF}(t) = \frac{1}{\Delta t} \int d^3 r I(\mathbf{r}) \sum_{s,k} \frac{e^{\lambda_s \Delta t} - 1}{\lambda_s} X_{4s} X_{sk}^{-1} \delta C_k(\mathbf{r}, t) \quad (28)$$

and obtain

$$\begin{aligned} \langle \delta \bar{N}_{CaF}(t) \delta \bar{N}_{CaF}(0) \rangle &= \frac{1}{\Delta t^2} \int d^3 r I(\mathbf{r}) \int d^3 r' I(\mathbf{r}') \left( \sum_{s,k,\ell,j} \frac{e^{\lambda_s \Delta t} - 1}{\lambda_s} \frac{e^{\lambda_\ell \Delta t} - 1}{\lambda_\ell} X_{4\ell} X_{\ell j}^{-1} X_{4s} X_{sk}^{-1} \langle \delta C_k(\mathbf{r}, t) \delta C_j(\mathbf{r}', 0) \rangle \right) \\ &= \frac{1}{\Delta t^2} \sum_{s,k,\ell,j} \frac{e^{\lambda_s \Delta t} - 1}{\lambda_s} \frac{e^{\lambda_\ell \Delta t} - 1}{\lambda_\ell} X_{4\ell} X_{\ell j}^{-1} X_{4s} X_{sk}^{-1} \langle \delta N_k(t) \delta N_j(0) \rangle \\ &\approx \langle \delta N_4(t) \delta N_4(0) \rangle + \sum_{s,k,\ell,j} \frac{\lambda_s \Delta t}{2} \frac{\lambda_\ell \Delta t}{2} X_{4\ell} X_{\ell j}^{-1} X_{4s} X_{sk}^{-1} \langle \delta N_k(t) \delta N_j(0) \rangle, \end{aligned} \quad (29)$$

where  $\delta N_k(t) = \int d^3 r I(\mathbf{r}) \delta C_k(\mathbf{r}, t)$  is the instantaneous fluctuation in the number of particles of species  $k$  in the observation volume. This implies that, in principle, the ACF is a superposition of the ACF of the fluctuations in the particle number of all the species that affect the time evolution of the observed variable ( $C_4$  in our case) and, also, of cross correlations. Extending this computation to the space-dependent problem of interest (with diffusion) would also yield a weighted sum of these correlations. Equations (26) and (29) reflect that, by adding the fluctuations in the particle numbers over a finite time, the finite time correlation between fluctuations in the observed variable ( $\bar{N}_{Ca^{2+}}$ ) and in the particle number of the other species can be present in the ACF. It is important to note that the correlation times are always the ones determined by the linearized reaction-diffusion system. The correction derived in this section implies that the timescales might be present with weights that are different from those prescribed by the usual theory in which Eq. (15) is assumed to hold for the fluctuations averaged over the finite acquisition time. The correction would be more or less relevant depending on the parameters of the acquisition time, the eigenvalues, weights, and relative concentrations.

## V. COMPARISON BETWEEN THEORY AND EXPERIMENTS

In this section the theory is applied to explain the experimental results of [32]. It is further illustrated with additional experimental results performed in aqueous solutions with  $Ca^{2+}$ , EGTA, and a different  $Ca^{2+}$  dye from the one used in Ref. [32].

For the parameters of Table I and, consequently, for the experiments of [32], it is reasonable to assume that  $N_{Ca^{2+}}$  and  $N_{FT}$  are independent. In particular, in the observation volume,  $V_{ef} \approx 0.6 \mu m^3$ , the mean number of reactions during the experimental acquisition time ( $\Delta t = 20 \mu s$ ) between  $Ca^{2+}$  and F is very small compared to the mean,  $\langle N_{Ca^{2+}} \rangle$  (e.g.,  $\sim 0.6$  vs  $\langle N_{Ca^{2+}} \rangle \sim 1300$  ions for the experiment with  $[Ca^{2+}]_{tot} = 9.27 \mu M$ ). Changes in the stochastic variable,  $N_{Ca^{2+}}$ , are therefore mostly determined by diffusion of the free  $Ca^{2+}$  ions in and out of the volume ( $\sim 226$  crossings during the experimental acquisition time for  $[Ca^{2+}]_{tot} = 9.27 \mu M$ ) and by the reactions between  $Ca^{2+}$  and the EGTA molecules ( $\sim 51$  reactions in  $V_{ef}$  during  $\Delta t$  for  $[Ca^{2+}]_{tot} = 9.27 \mu M$ ). On the other hand, due to the relatively large free diffusion coefficient of the ions it is reasonable to assume that  $N_{Ca^{2+}}$  is almost Poissonian [37], so that its variance is equal to its mean. This implies that, for the experimental conditions of [32], the only relevant correction in the space-dependent version of Eq. (29) would be the one due to the ACF of the fluctuations in the number of free  $Ca^{2+}$  ions. In fact, the observations of [32] can be explained assuming that the ACF can be written as

$$\begin{aligned} G(\tau) &= \frac{1}{([CaF]_{eq} V_{ef})^2} [\tilde{G}_{CaF}(\tau) + \alpha \tilde{G}_{Ca^{2+}}(\tau)] \\ &= \frac{1}{([CaF]_{eq} V_{ef})^2} \int d^3 r d^3 r' Q^2 I(r) I(r') \{ \langle \delta [CaF](\mathbf{r}, t) \times \delta [CaF](\mathbf{r}', t + \tau) \rangle + \alpha \langle \delta [Ca^{2+}](\mathbf{r}, t) \times \delta [Ca^{2+}](\mathbf{r}', t + \tau) \rangle \}, \end{aligned} \quad (30)$$

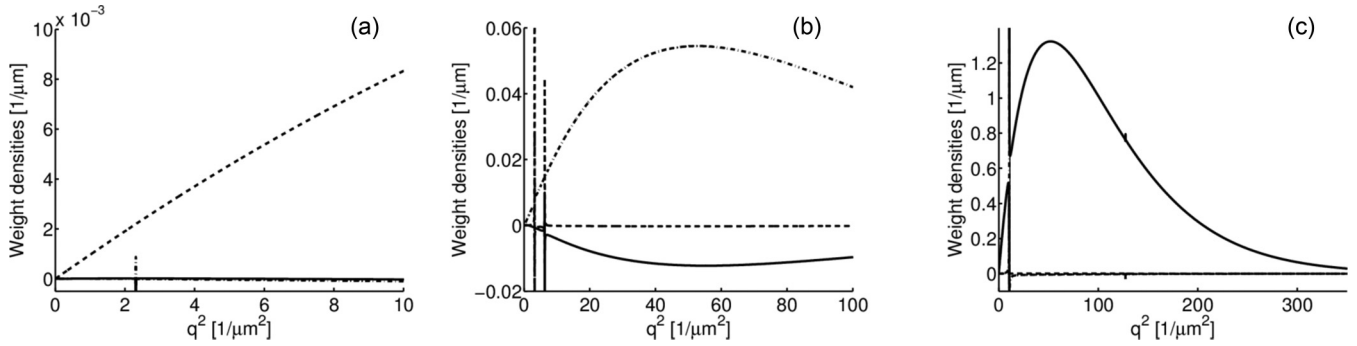


FIG. 6. Weight densities of the three components of  $G_{\text{Ca}^{2+}}$  computed as functions of  $q^2$  at  $\varphi = \pi/2$ . Symbols and  $[\text{Ca}^{2+}]_{\text{tot}}$  in (a)–(c) are the same as in Fig. 1.

with  $\alpha > 0$  and  $\tilde{G}_{\text{CaF}}(\tau) \equiv \langle \delta N_{\text{CaF}}(\tau) \delta N_{\text{CaF}}(0) \rangle$  and  $\tilde{G}_{\text{Ca}^{2+}}(\tau) \equiv \langle \delta N_{\text{Ca}^{2+}}(\tau) \delta N_{\text{Ca}^{2+}}(0) \rangle$  computed with the usual assumption on the instantaneous correlations [i.e.,  $\tilde{G}_{\text{CaF}}(\tau)$  is the first term of an expansion like the one in the right-hand side (RHS) of Eq. (29) and  $\tilde{G}_{\text{Ca}^{2+}}(\tau)$  would be one of the other terms]. Given that  $\tilde{G}_{\text{CaF}}(0) = \text{Var}(N_{\text{CaF}}) = \langle N_{\text{CaF}} \rangle$  and  $\tilde{G}_{\text{Ca}^{2+}}(0) = \text{Var}(N_{\text{Ca}^{2+}}) = \langle N_{\text{Ca}^{2+}} \rangle$ , Eq. (30) reduces to Eq. (19) for  $\tau = 0$ . Thus Eq. (30) is consistent with the assumptions that  $N_{\text{Ca}^{2+}}$  and  $N_{\text{FT}}$  are independent and that  $N_{\text{CaF}}$  is Poisson distributed.

$\tilde{G}_{\text{CaF}}$  and  $\tilde{G}_{\text{Ca}^{2+}}$  in Eq. (30) can be written as the sum of components, each one associated to an eigenvalue branch of the linearization of Eqs. (A1). Due to the structure of the corresponding eigenvectors,  $\tilde{G}_{\text{Ca}^{2+}}$  only depends on the nontrivial eigenvalues, i.e., it is the sum of three components. We show in Fig. 6 the corresponding weight densities for the same conditions and with the same selection of symbols as in Fig. 1 ( $[\text{Ca}^{2+}]_{\text{tot}} = 9300 \mu\text{M}$  in (a),  $[\text{Ca}^{2+}]_{\text{tot}} = 9600 \mu\text{M}$  in (b), and  $[\text{Ca}^{2+}]_{\text{tot}} = 10400 \mu\text{M}$  in (c)). It can be observed that the component of largest weight density is the one corresponding to  $\lambda_2$  in (a), to  $\lambda_3$  in (b), and to  $\lambda_1$  in (c). Comparing

Figs. 6 and 1 it is possible to conclude that the largest weight density attains its maximum value for a wave number,  $q$ , such that  $d\lambda_2/dq^2 \sim -D_E$  for the conditions of Fig. 6(a),  $d\lambda_3/dq^2 \sim -D_{\text{Ca}^{2+}} \sim -D_{ef2}$  for the conditions of Fig. 6(b), and  $d\lambda_1/dq^2 \sim -D_E$  for the conditions of Fig. 6(c). The coefficients,  $D_E$ ,  $D_{ef2}$ , and  $D_E$  were the ones obtained from the fittings of [32], besides the free diffusion coefficient of the dye,  $D_F$ , for the  $\text{Ca}^{2+}$  concentrations of Figs. 6(a)–6(c), respectively.

In order to further illustrate that it is in fact possible to estimate correctly the diffusion coefficients of nonfluorescent species performing FCS experiments in reaction-diffusion systems, we repeated the experiments of [32] in aqueous solutions with  $\text{Ca}^{2+}$ , EGTA, and the  $\text{Ca}^{2+}$  dye, Fluo8, instead of Fluo4. Fluo8 differs from Fluo4 in its off rate and dissociation constant ( $k'_F = 47.52 \text{ s}^{-1}$  and  $K_{dF} = 0.432 \mu\text{M}$  instead of  $300 \text{ s}^{-1}$  and  $2.6 \mu\text{M}$ , respectively) and in its free diffusion coefficient ( $D_F = 109 \mu\text{m}^2/\text{s}$  instead of  $85 \mu\text{m}^2/\text{s}$ ). The experiments were performed using  $[\text{F}]_{\text{tot}} = 0.676 \mu\text{M}$ ,  $[\text{E}]_{\text{tot}} = 9.66 \text{ mM}$ , and the total  $\text{Ca}^{2+}$  concentrations: 9.27, 9.37, 9.42, 9.52, 9.57, 9.61, and 9.66 mM. The best fits

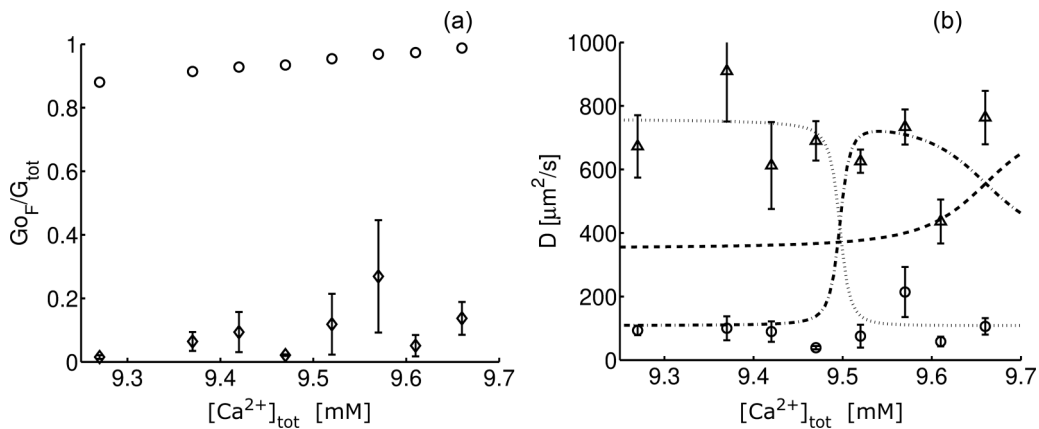


FIG. 7. Theoretical and experimental results (with lines and symbols, respectively) for the case of experiments performed in aqueous solutions containing  $\text{Ca}^{2+}$ , EGTA, and Fluo8. The theoretical results were obtained using the corresponding parameters of Table 1 with  $D_E = 352 \mu\text{m}^2$ . (a) Ratio between the weight associated to the free diffusion coefficient of the dye and the total weight of the ACF derived from the experiments [ $G_{\text{OF}}/G_{\text{tot}} = A_{1,\text{fit}}/(A_{1,\text{fit}} + A_{1,\text{fit}})$ ; rhombuses with error bars] and computed as in Fig. 2(c) ( $G_{\text{OF}}/G_{\text{tot}} = A_4/G_{\text{tot}}$ ; circles). (b) Effective diffusion coefficients (dashed line:  $D_{ef1}$ ; dash-dotted line:  $D_{ef2}$ ; dotted line:  $D_{ef3}$ ) and coefficients derived by fitting the experimental ACFs with expressions of the form Eq. (31) for each  $[\text{Ca}^{2+}]_{\text{tot}}$  probed, circles for the diffusion coefficient derived from  $\tau_1$ , and triangles for the one derived from  $\tau_2$ . The experimental points correspond to averages over three experiments for almost all values of  $[\text{Ca}^{2+}]_{\text{tot}}$ , two for  $[\text{Ca}^{2+}]_{\text{tot}} = 9.37$  and  $9.57$ , and six for  $[\text{Ca}^{2+}]_{\text{tot}} = 9.66 \text{ mM}$ .

corresponded to an expression of the form

$$G_{\text{fit}}(\tau) \approx \frac{A_{1,\text{fit}}}{\left(1 + \frac{\tau}{\tau_1}\right)\sqrt{1 + \frac{\tau}{w^2\tau_1}}} + \frac{A_{2,\text{fit}}e^{-\nu\tau}}{\left(1 + \frac{\tau}{\tau_2}\right)\sqrt{1 + \frac{\tau}{w^2\tau_2}}}, \quad (31)$$

with  $\tau_1$  equal to the diffusion timescale of the dye for all concentrations. Figure 7(a) shows the ratio between the weight associated to the free diffusion coefficient of the dye and the total weight of the ACF derived from the experiments [ $G_{\text{OF}}/G_{\text{tot}} = A_{1,\text{fit}}/(A_{1,\text{fit}} + A_{2,\text{fit}})$ : rhombuses with error bars] and the corresponding ratios predicted by the theory under the usual assumption on the instantaneous correlations ( $G_{\text{OF}}/G_{\text{tot}} = A_4/G_{\text{tot}}$ : circles). The theoretical results were computed as in Fig. 2(c), using the corresponding parameters of Table I with  $D_E = 352 \mu\text{m}^2$ . The fact that the experimental ratios are sensitively smaller than the theoretical ones can again be attributed to the miscalculation of the theoretical variance and, therefore, of the total weight, when the correlations due to the finite acquisition time are not included.

Figure 7(b) shows the effective diffusion coefficients (with lines) and those derived from the fitting (averages over two, three, or six experiments with symbols) as functions of  $[\text{Ca}^{2+}]_{\text{tot}}$ . It can be observed that, in almost all cases, one of the fitted coefficients corresponds to the free diffusion of the dye (circles) and the other to the largest effective diffusion coefficient of the problem (triangles), which is approximately equal to the free  $\text{Ca}^{2+}$  diffusion coefficient.

## VI. CONCLUSIONS

In this work the ACF of the fluctuations in the number of fluorescent molecules in an observation volume has been studied theoretically for the reaction-diffusion system composed of  $\text{Ca}^{2+}$ , a SW  $\text{Ca}^{2+}$  dye (Fluo4) that becomes fluorescent when bound to  $\text{Ca}^{2+}$ , and a  $\text{Ca}^{2+}$  chelator (EGTA). The study was done without making approximations based on the timescales involved. It showed that the eigenvalues that determine the correlation times of the ACF can be approximated by the sum of a diffusive and an exponential decay rate [as in Eq. (10)] with constant diffusion coefficients over finite wave number intervals for almost all wave numbers (Fig. 1). As expected, the diffusive and exponential rates corresponded to those prescribed by the fast reaction approximation for short enough wave numbers. The detailed analysis of the weights associated to these timescales showed that, under the usual assumptions on the instantaneous correlations of the molecule number fluctuations, the ACF should be characterized by a single diffusion coefficient: the one of the dye (Fig. 3). In any practical realization, *instantaneous* actually corresponds to a short time interval. The ACF was then computed including the finite experimental acquisition time which resulted in a function of all the timescales of the linearized reaction-diffusion system (Sec. IV). Based on the analysis of Sec. III, this implies that the ACF should be characterized by diffusive timescales that correspond to the effective or free diffusion coefficients of the species of the system, depending on the parameters. The presence of these timescales reconciled the theory with the experimental results of [32]. It also has the important consequence that the diffusion coefficients of nonfluorescent species can, in principle, be drawn from FCS experiments per-

formed in reaction-diffusion systems. This ability to quantify such diffusion coefficients was further validated with experiments in Sec. V.

The conclusion derived in Sec. III B, according to which the ACF of the fluorescence fluctuations for the system of  $\text{Ca}^{2+}$ , Fluo4, and EGTA should only depend on the diffusion coefficient of the dye, contradicted the experimental observations of [32]. Namely, in Ref. [32] other diffusive timescales of the system could be estimated correctly with FCS experiments. Another inconsistency between theory and experiments was the mismatch between the total weight of the experimental ACF and its expected value computed using Eq. (12), the experimental concentrations, and the dissociation constants provided by the vendors (see Fig. 3 in Ref. [32]). This discrepancy was solved in Sec. IV B by including the dependence of the variance of the number of fluorescent molecules in the observation volume,  $N_{\text{CaF}}$ , on the variance of the number of free  $\text{Ca}^{2+}$  ions,  $N_{\text{Ca}^{2+}}$ , in the same volume. To this end, the variance decomposition formula was used. The theoretical arguments were complemented with stochastic simulations (Fig. 5). It was shown in Sec. IV C that the dependence between the variance of  $N_{\text{CaF}}$  and that of  $N_{\text{Ca}^{2+}}$  was a consequence of the finite acquisition time during which the information on these stochastic variables is collected in experiments. The computation of the ACF with Eq. (20) showed that the finite acquisition time can introduce several new terms in the function [see Eq. (27) for the case with wavelength independent eigenvalues]. Arguing that, for the parameters of the experiments in Ref. [32], it was reasonable to assume that the number of free  $\text{Ca}^{2+}$  ions,  $N_{\text{Ca}^{2+}}$ , and the total number of dye molecules,  $N_{\text{FT}}$ , were independent and that  $N_{\text{Ca}^{2+}}$  was Poisson distributed, only the term associated to the ACF of the free  $\text{Ca}^{2+}$  ions was kept. With this additional term the experimental results of [32] were explained in Sec. V. Namely, it was shown that the diffusive timescales that could be estimated correctly in Ref. [32] corresponded to the eigenvalues with the largest weight density of the ACF,  $\tilde{G}_{\text{Ca}^{2+}}(\tau) = \langle \delta N_{\text{Ca}^{2+}}(\tau) \delta N_{\text{Ca}^{2+}}(0) \rangle$ , of the number of free  $\text{Ca}^{2+}$  ions, for each of the conditions probed experimentally. In Sec. V, the results of experiments performed with the  $\text{Ca}^{2+}$  dye, Fluo8, which differs in its kinetics and diffusion coefficient from the one used in Ref. [32], were presented. These results again displayed the mismatch between the experimental weights of the ACF and those prescribed by the theory under the usual assumption on the instantaneous correlations [Fig. 7(a)]. The experiments allowed the correct quantification of the diffusion coefficient of a nonfluorescent species (the free  $\text{Ca}^{2+}$  ions) as shown in Fig. 7(b). The identification of the timescales that are obtained in these experiments is a necessary step for the use of SW dyes in FCS experiments performed in living cells to quantify the transport properties of free  $\text{Ca}^{2+}$  in this setting (work in progress).

The results of the theory presented in this paper also apply to FCS experiments performed in systems with other types of fluorescent species, e.g., those done in *Drosophila melanogaster* embryos expressing the fluorescent protein, Bcd-EGFP [38]. The interpretation of the timescales drawn from these experiments [9,39] in terms of an underlying reaction-diffusion system under the fast reaction approximation gave estimates of various biophysical parameters [10] that

proved to be consistent with other observations [35,40]. The agreement held even if the relative weights of the experimental ACF components differed from the theoretical ones [36]. The correct quantification of the biophysical parameters of the system in this example can now be explained in terms of the theory developed in the present paper.

In summary, the work in this paper has shown that the finite acquisition time, which is unavoidable in any practical implementation of FCS, affects the weights and the correlation times that characterize the ACF of the fluorescence fluctuations in reaction-diffusion systems. It affects it in such a way that the transport rates of the nonfluorescent species can be derived from the correlation times. The results not only provide theoretical support for the quantification of biophysical parameters from FCS experiments presented in previous works, they also suggest that the acquisition time is an experimental tool to probe more thoroughly the timescales that characterize the dynamics of reaction-diffusion systems with FCS experiments.

### ACKNOWLEDGMENTS

This research has been supported by UBA (Grant No. UBACyT 20020170100482BA) and ANPCyT (Grants No. PICT 2015-3824 and No. PICT 2018-02026). S.P.D. acknowledges support as a member of Carrera del Investigador Científico (Consejo Nacional de Investigaciones Científicas y Técnicas). S.P.D. acknowledges the hospitality of the ICTP in Trieste, Italy.

### APPENDIX

#### 1. Reaction-diffusion system

The evolution equations for the reaction-diffusion system with  $\text{Ca}^{2+}$ , a  $\text{Ca}^{2+}$  dye, F, and a  $\text{Ca}^{2+}$  chelator, E, that react according to Eqs. (2) are

$$\begin{aligned} \frac{\partial [\text{E}]_{\text{tot}}}{\partial t} &= D_E \nabla^2 [\text{E}], \\ \frac{\partial [\text{F}]_{\text{tot}}}{\partial t} &= D_F \nabla^2 [\text{F}], \\ \frac{\partial [\text{CaE}]}{\partial t} &= D_E \nabla^2 [\text{CaE}] + k_E [\text{Ca}^{2+}] \\ &\quad \times ([\text{E}]_{\text{tot}} - [\text{CaE}]) - k'_E [\text{CaE}], \\ \frac{\partial [\text{CaF}]}{\partial t} &= D_F \nabla^2 [\text{CaF}] + k_F [\text{Ca}^{2+}] \\ &\quad \times ([\text{F}]_{\text{tot}} - [\text{CaF}]) - k'_F [\text{CaF}], \\ \frac{\partial [\text{Ca}^{2+}]}{\partial t} &= D_{\text{Ca}^{2+}} \nabla^2 [\text{Ca}^{2+}] - k_F [\text{Ca}^{2+}] \\ &\quad \times ([\text{F}]_{\text{tot}} - [\text{CaF}]) + k'_F [\text{CaF}] - k_E [\text{Ca}^{2+}] \\ &\quad \times ([\text{E}]_{\text{tot}} - [\text{CaE}]) + k'_E [\text{CaE}], \end{aligned} \quad (\text{A1})$$

where  $[\text{E}]_{\text{tot}} = [\text{E}] + [\text{CaE}]$ ,  $[\text{F}]_{\text{tot}} = [\text{F}] + [\text{CaF}]$ , and the free diffusion coefficients of the species are  $D_{\text{Ca}^{2+}}$  (for  $\text{Ca}^{2+}$ ),  $D_E$  (for E and CaE), and  $D_F$  (for F and CaF).

#### 2. Simplified ACF in the fast reaction limit

The fast reaction limit holds when the characteristic times of the reactions are shorter than the time it takes for the

species to diffuse across the observation volume. In such a case, Eq. (10) provides a good approximation of the nontrivial eigenvalues throughout the range of  $q$  values that contribute non-negligibly to their corresponding components. Under the assumption of Eq. (15) the ACF is then given by [32]

$$\begin{aligned} G(\tau) &= \frac{Go_F}{\left(1 + \frac{\tau}{\tau_{D_F}}\right) \sqrt{1 + \frac{\tau}{w^2 \tau_{D_F}}}} + \frac{Go_{ef1}}{\left(1 + \frac{\tau}{\tau_{D_{ef1}}}\right) \sqrt{1 + \frac{\tau}{w^2 \tau_{D_{ef1}}}}} \\ &\quad + \frac{Go_{ef2} e^{-\nu_{ef2} \tau}}{\left(1 + \frac{\tau}{\tau_{D_{ef2}}}\right) \sqrt{1 + \frac{\tau}{w^2 \tau_{D_{ef2}}}}} \\ &\quad + \frac{Go_{ef3} e^{-\nu_{ef3} \tau}}{\left(1 + \frac{\tau}{\tau_{D_{ef3}}}\right) \sqrt{1 + \frac{\tau}{w^2 \tau_{D_{ef3}}}}}, \end{aligned} \quad (\text{A2})$$

with  $\tau_{D_{efi}} = \frac{w^2}{4D_{efi}}$ , where the effective diffusion coefficients,  $D_{efi}$ , and the effective rates,  $\nu_{efi}$ , satisfy

$$D_{ef1} + D_{ef2} + D_{ef3} = D_{\text{Ca}^{2+}} + D_F + D_E, \quad (\text{A3})$$

$$\nu_{ef1} + \nu_{ef2} = \nu_F + \nu_E, \quad (\text{A4})$$

where  $\nu_F = k'_F([\text{F}]_{\text{eq}}/Kd_F + [\text{F}]_{\text{tot}}/[\text{F}]_{\text{eq}})$  and  $\nu_E = k'_E([\text{E}]_{\text{eq}}/Kd_E + [\text{E}]_{\text{tot}}/[\text{E}]_{\text{eq}})$  are related to the timescales when E and F are not part of the system, respectively. Thus, in this limit, the ACF has one purely diffusive component associated to the free diffusion coefficient of the dye and three more components (one of them purely diffusive as well) that depend on effective diffusion coefficients that are functions of the free coefficients,  $D_F$ ,  $D_{\text{Ca}^{2+}}$ , and  $D_E$ , the concentrations, and the reaction rates. In Ref. [32] we could fit the ACF derived from FCS experiments performed in aqueous solutions containing  $\text{Ca}^{2+}$ , the  $\text{Ca}^{2+}$  dye, Fluo4 dextran, and the  $\text{Ca}^{2+}$  buffer, EGTA, using two purely diffusive components:

$$G_{\text{fit}}(\tau) \approx \frac{A_{1,\text{fit}}}{\left(1 + \frac{\tau}{\tau_1}\right) \sqrt{1 + \frac{\tau}{w^2 \tau_1}}} + \frac{A_{2,\text{fit}}}{\left(1 + \frac{\tau}{\tau_2}\right) \sqrt{1 + \frac{\tau}{w^2 \tau_2}}}. \quad (\text{A5})$$

The experiments of [32] were performed for different total concentrations of  $\text{Ca}^{2+}$ ,  $[\text{Ca}^{2+}]_{\text{tot}}$ . Analyzing the  $[\text{Ca}^{2+}]$  dependence of the fitted coefficients,  $D_i$ ,  $i = 1, 2$ , we identified the  $[\text{Ca}^{2+}]$ -invariant one with the free diffusion coefficient of the dye,  $D_F$  [32]. Comparing the  $[\text{Ca}^{2+}]$  dependence of the other with what the fast reaction limit prescribed for the three effective diffusion coefficients that enter the ACF, Eq. (A2), allowed us to give it an interpretation (that was different depending on the range of  $[\text{Ca}^{2+}]_{\text{tot}}$ ) and eventually estimate the free diffusion coefficients,  $D_{\text{Ca}^{2+}}$  and  $D_E$ .

#### 3. Linearized reaction-diffusion system, eigenvalues, and eigenvectors

To compute the eigenvalue branches of Sec. II and their corresponding eigenvectors we first work with Eqs. (A1) linearized around the equilibrium solution written in terms of the following concentration differences:  $\xi_1 = [\text{E}]_{\text{tot}} - [\text{E}]_{\text{tot,eq}}$ ,  $\xi_2 = [\text{F}]_{\text{tot}} - [\text{F}]_{\text{tot,eq}}$ ,  $\xi_3 = [\text{CaE}] - [\text{CaE}]_{\text{eq}}$ ,  $\xi_4 = [\text{CaF}] - [\text{CaF}]_{\text{eq}}$ , and  $\xi_5 = [\text{Ca}^{2+}] - [\text{Ca}^{2+}]_{\text{eq}}$ . We then Fourier transform the variables in space and rewrite the evolution equation

as  $\hat{\xi}(q) = A(q)\hat{\xi}(q)$  with  $\hat{\xi}(q)$  the vector of Fourier transformed components,  $\hat{\xi}_1(q), \dots, \hat{\xi}_5(q)$  as functions of the wave number,  $q$ , and the matrix,  $A(q)$ , given by

$$A(q) = \begin{pmatrix} -D_E q^2 & 0 & 0 & 0 & 0 \\ 0 & -D_F q^2 & 0 & 0 & 0 \\ k_E[\text{Ca}^{2+}]_{eq} & 0 & -k'_E - k_E[\text{Ca}^{2+}]_{eq} - D_E q^2 & 0 & k_E[\text{E}]_{eq} \\ 0 & k_F[\text{Ca}^{2+}]_{eq} & 0 & -k'_F - k_F[\text{Ca}^{2+}]_{eq} - D_F q^2 & k_F[\text{F}]_{eq} \\ -k_E[\text{Ca}^{2+}]_{eq} & -k_F[\text{Ca}^{2+}]_{eq} & k'_E + k_E[\text{Ca}^{2+}]_{eq} & k'_F + k_F[\text{Ca}^{2+}]_{eq} & -k_E[\text{E}]_{eq} - k_F[\text{F}]_{eq} - D_{\text{Ca}^{2+}} q^2 \end{pmatrix}. \quad (\text{A6})$$

The eigenvalues,  $\lambda_i(q)$ , of  $A(q)$  give the eigenvalue branches we referred to in Sec. II. Clearly,  $\lambda_4$  and  $\lambda_5$  of Eqs. (7) and (8) are eigenvalues of this matrix. In this basis, the eigenvectors can be readily computed in terms of the eigenvalues and other parameters of the problems. Once we have them, we switch to the basis defined by the Fourier transform of the concentration differences,  $c_1 = [\text{E}] - [\text{E}]_{eq}$ ,  $c_2 = [\text{F}] - [\text{F}]_{eq}$ , and  $c_k = \xi_k$  for  $k = 3, 4, 5$ , so that we can assume that only one of them is fluorescent,  $c_4 = [\text{CaF}] - [\text{CaF}]_{eq}$ . Clearly,  $c_1 = \xi_1 - \xi_3$  and  $c_2 = \xi_2 - \xi_4$ . The eigenvector matrix,  $M(q)$  (with the eigenvectors as columns), and the change of basis,  $B(q)$ , such that  $\hat{c}(q) = B(q)\hat{\xi}(q)$ , are given by

$$M(q) = \begin{pmatrix} 0 & 0 & 0 & 0 & 1 \\ 0 & 0 & 0 & 1 & 0 \\ w & r & s & 0 & p \\ f & g & h & e & 0 \\ 1 & 1 & 1 & 0 & 0 \end{pmatrix}, \quad B(q) = \begin{pmatrix} 1 & 0 & -1 & 0 & 0 \\ 0 & 1 & 0 & -1 & 0 \\ 0 & 0 & 1 & 0 & 0 \\ 0 & 0 & 0 & 1 & 0 \\ 0 & 0 & 0 & 0 & 1 \end{pmatrix}, \quad (\text{A7})$$

with  $w = k_E[\text{E}]_{eq}/(k_E[\text{E}]_{eq} + D_E q^2 + \lambda_1)$ ,  $r = k_E[\text{E}]_{eq}/(k_E[\text{E}]_{eq} + D_E q^2 + \lambda_2)$ ,  $s = k_E[\text{E}]_{eq}/(k_E[\text{E}]_{eq} + D_E q^2 + \lambda_3)$ ,  $p = k_E[\text{Ca}^{2+}]_{eq}/(k_E[\text{Ca}^{2+}]_{eq} + k'_E)$ ,  $f = k_F[\text{F}]_{eq}/(k_F[\text{F}]_{eq} + D_F q^2 + \lambda_1)$ ,  $g = k_F[\text{F}]_{eq}/(k_F[\text{F}]_{eq} + D_F q^2 + \lambda_2)$ ,  $h = k_F[\text{F}]_{eq}/(k_F[\text{F}]_{eq} + D_F q^2 + \lambda_3)$ , and  $e = k_F[\text{Ca}^{2+}]_{eq}/(k_F[\text{Ca}^{2+}]_{eq} + k'_F)$ . An analytic expression for the inverse of  $M$  in terms of these variables and of the eigenvalues can be obtained from  $M$  using algebraic manipulating software.

#### 4. Weight computation

We compute the nontrivial eigenvalues of  $A(q)$  as functions of  $q$  numerically. We then compute the eigenvector matrix  $M(q)$  and its inverse as functions of  $q$  [using Eq. (A7) and the corresponding one for  $M^{-1}$ ]. We follow [31] to compute  $G_{\text{CaF}}$  and  $G_{\text{Ca}^{2+}}$  in Eq. (30). Namely, we assume that

$$\langle c_s(\mathbf{r}, t) c'_s(\mathbf{r}', t) \rangle_{(pb)} = \frac{\delta(\mathbf{r} - \mathbf{r}')}{V_{ef}} \delta_{ss'} \text{Var}(N_s)_{(pb)} = \delta(\mathbf{r} - \mathbf{r}') \delta_{ss'} C_{s,eq}, \quad (\text{A8})$$

where  $C_{s,eq}$  is the equilibrium concentration of the  $s$ th species. In this way, it is

$$G_{\text{CaF}}(\tau) = \frac{1}{([\text{CaF}]_{eq} V_{ef})^2} \int d^3 q \left( \frac{|\hat{I}(q)|}{I(0)} \right)^2 \sum_{i,j,\ell=1}^5 B_{s\ell} M_{\ell i} e^{-\lambda_i(q)\tau} (M^{-1})_{ij} (B^{-1})_{js} C_{s,eq}, \quad s = 4, \quad (\text{A9})$$

with  $\hat{I}(q)$  the Fourier transform of  $I(r)$ , given by Eq. (4).  $G_{\text{Ca}^{2+}}$  has the same expression but with  $s = 5$  instead of 4. In this way, weight densities ( $i = 1, \dots, 4$ ) of  $G_{\text{CaF}}$  and  $G_{\text{Ca}^{2+}}$  can be written, respectively, as

$$g_{\text{CaF},i}(q) = \frac{q^2 [\text{CaF}]_{eq}}{(2\pi [\text{CaF}]_{eq})^2} \exp \left[ - \left( \frac{w_r q \sin(\varphi)}{2} \right)^2 - \left( \frac{w_z q \cos(\varphi)}{2} \right)^2 \right] \sum_{j,\ell=1}^5 B_{4\ell} M_{\ell i} (M^{-1})_{ij} (B^{-1})_{j4}, \quad (\text{A10})$$

$$g_{\text{Ca},i}(q) = \frac{q^2 [\text{Ca}^{2+}]_{eq}}{(2\pi [\text{Ca}^{2+}]_{eq})^2} \exp \left[ - \left( \frac{w_r q \sin(\varphi)}{2} \right)^2 - \left( \frac{w_z q \cos(\varphi)}{2} \right)^2 \right] \sum_{j,\ell=1}^5 B_{5\ell} M_{\ell i} (M^{-1})_{ij} (B^{-1})_{j5}. \quad (\text{A11})$$

The weights,  $A_i$ , of Fig. 2 are computed integrating the weights,  $g_i$ , of Eq. (A10) over  $q$  and  $\varphi$  as in Eq. (13).

### 5. Variance decomposition

We consider the conditional probability,  $P(N_{\text{CaF}} | N_{\text{Ca}^{2+}}, N_{\text{FT}})$  that  $N_{\text{CaF}}$  takes a certain value given that  $N_{\text{Ca}^{2+}}$  and  $N_{\text{FT}}$  take some other values and write

$$\begin{aligned}
 \text{Var}(N_{\text{CaF}}) &= \sum_{N_{\text{CaF}}, N_{\text{Ca}^{2+}}, N_{\text{FT}}} (N_{\text{CaF}} - \langle N_{\text{CaF}} \rangle)^2 P(N_{\text{CaF}} | N_{\text{Ca}^{2+}}, N_{\text{FT}}) P(N_{\text{Ca}^{2+}}) P(N_{\text{FT}}) \\
 &= \sum_{N_{\text{Ca}^{2+}}} \left( P(N_{\text{Ca}^{2+}}) \sum_{N_{\text{CaF}}, N_{\text{FT}}} (N_{\text{CaF}} - \langle N_{\text{CaF}} | N_{\text{Ca}^{2+}} \rangle)^2 P(N_{\text{CaF}} | N_{\text{Ca}^{2+}}, N_{\text{FT}}) P(N_{\text{FT}}) \right) \\
 &\quad + \sum_{N_{\text{Ca}^{2+}}} \left( P(N_{\text{Ca}^{2+}}) \sum_{N_{\text{CaF}}, N_{\text{FT}}} (\langle N_{\text{CaF}} | N_{\text{Ca}^{2+}} \rangle - \langle N_{\text{CaF}} \rangle)^2 P(N_{\text{CaF}} | N_{\text{Ca}^{2+}}, N_{\text{FT}}) P(N_{\text{FT}}) \right) \\
 &\quad + 2 \sum_{N_{\text{Ca}^{2+}}} \left( P(N_{\text{Ca}^{2+}}) (\langle N_{\text{CaF}} | N_{\text{Ca}^{2+}} \rangle - \langle N_{\text{CaF}} \rangle) \sum_{N_{\text{CaF}}, N_{\text{FT}}} (N_{\text{CaF}} - \langle N_{\text{CaF}} | N_{\text{Ca}^{2+}} \rangle) P(N_{\text{CaF}} | N_{\text{Ca}^{2+}}, N_{\text{FT}}) P(N_{\text{FT}}) \right),
 \end{aligned} \tag{A12}$$

where

$$\begin{aligned}
 \langle N_{\text{CaF}} | N_{\text{Ca}^{2+}} \rangle &= \sum_{N_{\text{CaF}}, N_{\text{FT}}} N_{\text{CaF}} P(N_{\text{CaF}} | N_{\text{Ca}^{2+}}, N_{\text{FT}}) P(N_{\text{FT}}), \\
 \langle N_{\text{CaF}} \rangle &= \sum_{N_{\text{CaF}}, N_{\text{Ca}^{2+}}, N_{\text{FT}}} N_{\text{CaF}} P(N_{\text{CaF}} | N_{\text{Ca}^{2+}}, N_{\text{FT}}) P(N_{\text{Ca}^{2+}}) P(N_{\text{FT}}).
 \end{aligned} \tag{A13}$$

The last line in Eq. (A12) clearly cancels out and we rewrite the other two sums as in Eq. (17) with

$$\begin{aligned}
 \langle \text{Var}(N_{\text{CaF}} | N_{\text{Ca}^{2+}}) \rangle_{N_{\text{Ca}^{2+}}} &= \sum_{N_{\text{Ca}^{2+}}} \left( P(N_{\text{Ca}^{2+}}) \sum_{N_{\text{CaF}}, N_{\text{FT}}} (N_{\text{CaF}} - \langle N_{\text{CaF}} | N_{\text{Ca}^{2+}} \rangle)^2 P(N_{\text{CaF}} | N_{\text{Ca}^{2+}}, N_{\text{FT}}) P(N_{\text{FT}}) \right), \\
 \text{Var}_{N_{\text{Ca}^{2+}}}(\langle N_{\text{CaF}} | N_{\text{Ca}^{2+}} \rangle) &= \sum_{N_{\text{Ca}^{2+}}} \left( P(N_{\text{Ca}^{2+}}) \sum_{N_{\text{CaF}}, N_{\text{FT}}} (\langle N_{\text{CaF}} | N_{\text{Ca}^{2+}} \rangle - \langle N_{\text{CaF}} \rangle)^2 P(N_{\text{CaF}} | N_{\text{Ca}^{2+}}, N_{\text{FT}}) P(N_{\text{FT}}) \right).
 \end{aligned} \tag{A14}$$

### 6. Experiments: Data acquisition, computation, and fitting of the experimental ACF

FCS experiments were performed in aqueous solution containing  $\text{Ca}^{2+}$ , EGTA, and the fluorescent single wavelength calcium indicator Fluo8 (Abcam). Solutions also contained 100 mM KCl, 30 mM MOPS, and were done at pH 7.2. Fluorescence records were obtained in a spectral confocal scanning microscope FluoView 1000 (Olympus, Tokyo, Japan), using a 60x oil immersion objective (UPlanSApo), NA 1.35, and a 115  $\mu\text{m}$  pinhole size. The sample, a 70  $\mu\text{l}$  drop of the chosen solution deposited on a coverslip, was illuminated with the 488 nm line of an argon laser with an excitation power of 6–10  $\mu\text{W}$ . Fluorescence was collected from a single point located at approximately 15  $\mu\text{m}$  from the coverslip, at a 50 kHz acquisition rate during  $\sim 180$  s (equivalently, 8 388 096 data points) in the [500–600] nm range with a photomultiplier detector. The confocal volume was calibrated using a solution containing 100 nM of fluorescein (Sigma, St. Louis, MO) in a buffer solution pH=9, assuming a diffusion coefficient of 425  $\mu\text{m}^2/\text{s}$  [41]. The lateral width resulting value was  $w_r = (0.277 \pm 0.005) \mu\text{m}$ , with  $w = w_z/w_r = 5$  and the estimated effective volume was  $V_{\text{ef}} = (0.59 \pm 0.1) \mu\text{m}^3$ . Experimental ACFs were calculated with a custom-made routine written on the Matlab platform [42]. To this end, each 180 s long record was divided into

$N = 1021$ , 164 ms long segments containing  $2^{13}$  points each. The ACF was computed for each of the  $N = 1021$  segments, as mentioned in Ref. [32], from which the average ACF was obtained. The averaged ACFs were fitted with different combinations of Eq. (A2) components and the function *nlinfit* that comes with Matlab, using the default options [42]. The first 1–2 points were discarded; this sets a timelag range from 40–60  $\mu\text{s}$  to 164 ms. In each case we tried several initial guesses and chose the one that gave the smallest  $\chi^2$  given by

$$\chi^2 = \frac{1}{N_p - N_v} \sum_i^{N_p} \frac{[G_{\text{theo}}(\tau_i) - G_{\text{exp}}(\tau_i)]^2}{G_{\text{theo}}(\tau_i)}, \tag{A15}$$

with  $N_p$  the total number of data points of the experimental ACF,  $G_{\text{exp}}$ , and  $N_v$  the number of variables of the model  $G_{\text{theo}}$  the ACF computed with the fitting model.

### 7. Stochastic simulations

We perform stochastic simulations of the reaction-diffusion system assuming that particles move on a cubic grid of  $N = 30$  points per side with mesh size  $dx = dy = dz = 0.1 \mu\text{m}$ . Diffusion is simulated as random walk on the grid and the time step,  $dt \approx 2 \times 10^{-6}$  s, is chosen so as to accommodate the fastest diffusing species ( $\text{Ca}^{2+}$ , with

$D_{\text{Ca}^{2+}} = 760 \mu\text{m}^2/\text{s}$ ). In the full reaction-diffusion system simulation, reactions are performed going through all the pairs that can be formed at each time step and grid point and deciding with a certain probability whether the reaction occurs or not. We also perform simulations in which we only follow the  $\text{Ca}^{2+}$ -bound and  $\text{Ca}^{2+}$ -free dye molecules and where the transformation between these two species occurs with a fixed probability per unit time in both directions (proportional to the equilibrium  $\text{Ca}^{2+}$  concentration in the case that represents

binding with a constant  $k_{\text{off}}$  in the opposite case). In order to compute the number of molecules or ions of a given species within the observation volume we proceed as in Ref. [35]. Namely, we add all the particles but with a weight that is a Gaussian function of the distance to the center of the simulation volume with a width equivalent to that of the observation volume ( $w_x = 0.28 \mu\text{m}$  in  $x$  and  $y$  and  $w_z = 5w_x$  in the  $z$  direction). We also tried other ways of counting molecules, but we only present the results obtained in this way.

- 
- [1] D. Magde, E. Elson, and W. W. Webb, *Phys. Rev. Lett.* **29**, 705 (1972).
- [2] K. Berland, P. So, and E. E. Gratton, *Biophys. J.* **68**, 694 (1995).
- [3] N. L. Thompson, in *Topics in Fluorescence Spectroscopy: Techniques*, edited by J. R. Lakowicz (Springer US, Boston, MA, 1999), pp. 337–378.
- [4] S. A. Kim and P. Schuille, *Curr. Opin. Neurobiol.* **13**, 583 (2003).
- [5] E. Haustein and P. Schuille, *Annu. Rev. Biophys. Biomol. Struct.* **36**, 151 (2007).
- [6] E. L. Elson, *Traffic* **2**, 789 (2001).
- [7] D. Grünwald, M. C. Cardoso, H. Leonhardt, and V. Buschmann, *Curr. Pharm. Biotechnol.* **6**, 381 (2005).
- [8] L. Sigaut, M. L. Ponce, A. Colman-Lerner, and S. P. Dawson, *Phys. Rev. E* **82**, 051912 (2010).
- [9] A. Abu-Arish, A. Porcher, A. Czerwonka, N. Dostatni, and C. Fradin, *Biophys. J.* **99**, L33 (2010).
- [10] L. Sigaut, J. E. Pearson, A. Colman-Lerner, and S. Ponce Dawson, *PLoS Comput. Biol.* **10**, e1003629 (2014).
- [11] M. J. Berridge, M. D. Bootman, and P. Lipp, *Nature (London)* **395**, 645 (1998).
- [12] M. J. Berridge, P. Lipp, and M. D. Bootman, *Nat. Rev. Mol. Cell Biol.* **1**, 11 (2000).
- [13] G. Dupont, M. Falcke, V. Kirk, and J. Sneyd, *Models of Calcium Signalling* (Springer International Publishing, Berlin, 2016).
- [14] R. M. Paredes, J. C. Etzler, L. T. Watts, W. Zheng, and J. D. Lechleiter, *Methods (San Diego, Calif.)* **46**, 143 (2008).
- [15] M. C. Nowycky and A. P. Thomas, *J. Cell Sci.* **115**, 3715 (2002).
- [16] I. F. Smith, S. M. Wiltgen, J. Shuai, and I. Parker, *Sci. Signal* **2**, ra77 (2009).
- [17] S. Zeller, S. Rüdiger, H. Engel, J. Sneyd, G. Warnecke, I. Parker, and M. Falcke, *Biophys. J.* **97**, 992 (2009).
- [18] S. Weinberg and G. Smith, *Biophys. J.* **106**, 2693 (2014).
- [19] J. Shuai, J. E. Pearson, and I. Parker, *Biophys. J.* **95**, 3738 (2008).
- [20] D. Fraiman and S. P. Dawson, *Phys. Biol.* **11**, 016007 (2014).
- [21] J. D. Lechleiter and D. E. Clapham, *Cell* **69**, 283 (1992).
- [22] J. P. Keener and J. Sneyd, *Mathematical Physiology*, Interdisciplinary Applied Mathematics (Springer, New York, 1998).
- [23] B. Schwaller, *Cold Spring Harbor Perspect. Biol.* **2**, a004051 (2010).
- [24] N. Allbritton, T. Meyer, and L. Stryer, *Science* **258**, 1812 (1992).
- [25] B. Pando, S. P. Dawson, D.-O. D. Mak, and J. E. Pearson, *Proc. Natl. Acad. Sci. USA* **103**, 5338 (2006).
- [26] S. L. Dargan, B. Schwaller, and I. Parker, *J. Physiol.* **556**, 447 (2004).
- [27] E. Piegari, L. Sigaut, and S. P. Dawson, *Cell Calcium* **57**, 109 (2015).
- [28] E. Piegari, L. F. Lopez, and S. P. Dawson, *Phys. Biol.* **15**, 066006 (2018).
- [29] A. C. Ventura, L. Bruno, A. Demuro, I. Parker, and S. Ponce Dawson, *Biophys. J.* **88**, 2403 (2005).
- [30] L. Bruno, G. Solovey, A. C. Ventura, S. Dargan, and S. P. Dawson, *Cell Calcium* **47**, 273 (2010).
- [31] O. Krichevsky and G. Bonnet, *Rep. Prog. Phys.* **65**, 251 (2002).
- [32] L. Sigaut, C. Villarruel, and S. P. Dawson, *J. Chem. Phys.* **146**, 104203 (2017).
- [33] E. P. Ipiña and S. P. Dawson, *Phys. Rev. E* **87**, 022706 (2013).
- [34] L. Sigaut, C. Villarruel, M. L. Ponce, and S. Ponce Dawson, *Phys. Rev. E* **95**, 062408 (2017).
- [35] E. Pérez Ipiña and S. Ponce Dawson, *PLoS ONE* **13**, e0192091 (2018).
- [36] E. P. Ipiña and S. P. Dawson, *Biophys. J.* **107**, 2674 (2014).
- [37] C. Gardiner, *Handbook of Stochastic Methods for Physics, Chemistry and the Natural Sciences* (Springer, Berlin, 2004).
- [38] C. Fradin, *Biochim. Biophys. Acta, Proteins Proteomics* **1865**, 1676 (2017).
- [39] A. Porcher, A. Abu-Arish, S. Huart, B. Roelens, C. Fradin, and N. Dostatni, *Development* **137**, 2795 (2010).
- [40] E. P. Ipiña and S. P. Dawson, *Phys. Biol.* **14**, 016002 (2017).
- [41] C. T. Culbertson, S. C. Jacobson, and J. M. Ramsey, *Talanta* **56**, 365 (2002).
- [42] MATLAB, *version 7.10.0 (R2010a)* (The MathWorks Inc., Natick, MA, 2010).